

Constitutively optimal governing equations for higher-grade elastic beams

F. Amiot

*FEMTO-ST Institute, CNRS-UMR 6174 / UBFC / ENSMM / UTBM,
24 chemin de l'Épitaphe, F-25030 Besançon, France*

Abstract

A method is proposed herein to build beam equations for materials featuring higher-grade elasticity. As it is based on the minimization of the constitutive equation gap, static admissibility conditions are taken into account so that it naturally converges to the usual beam equations resulting from Cauchy elasticity when the beam dimensions are large enough. The method is exemplified, for Euler-Bernoulli beams, on first-strain gradient and second-strain gradient elasticity, which yield local and non-local beam equations, respectively. The solutions of these equations are computed for tensile and bending loads over a wide range of beam dimensions in order to assess the role of the different grades on the global behavior of simple mechanical structures. Under first-strain gradient elasticity, the proposed approach extends the validity of the equations obtained previously for tensile or bending loadings. Considering second-strain gradient elasticity, this additionally allows to distinguish two different regimes, depending on whether the elasticity is driven by the surface (it is proposed to denote this regime as the ecto-elastic regime) or by the bulk. It may also model the chemo-mechanical couplings. It finally suggests that second-strain gradient elasticity and first-strain gradi-

ent elasticity may affect the bending stiffness in the same dimensional range, so that both should always be considered simultaneously when analyzing experimental results.

Keywords:

beam theory, higher-grade elasticity, second-strain gradient elasticity, size-effect, constitutive equation gap, generalized continua

1. Introduction

Since the emergence of integrated circuits at the end of the 1950s as a response to the "tyranny of numbers", miniaturization has been a concern for the electrical engineering community, namely, being able to produce solid-state transistors was useless without the possibility to connect them efficiently and reliably. The wires between transistors were all soldered by hand, thus limiting both the increase in complexity and the reliability of the final device. The groundbreaking idea was to integrate the circuitry to the semi-conductor piece holding the transistors. It allowed the mass-production of reliable devices, and has been the starting point for successive technologies, all described by the "integration-level", measured as the number of transistors per chip, they allow: from small-scale integration (early 60s) to very-large-scale integration (80s). The technology was at that time mature enough to allow for other communities to benefit from the miniaturization possibilities. Non-electronic functions thus started to be integrated to the chips, and restricting to mechanical applications, this yielded devices such as pressure sensors, accelerometers, gyroscopes, microphones or ink-jet printer cartridges that are now on the market. The motivation was then mainly the

same as for electronic devices, namely, integration (all the above-mentioned mechanical devices are electrically read or driven), reliability and mass production.

These devices do not make use of any scale effect on the mechanical behavior of the fabricated objects, so that there is still room for innovative products making the most of the miniaturization capabilities. This however requires the development of modeling frameworks to pave the way for the engineering of these scale effects. Focusing on the mechanical behavior of solids, such scale effect encompass both size-dependent elasticity and surface couplings. Only few experimental results demonstrating size-dependent elasticity have been reported in the literature, mainly because of the difficulty to keep the experimental errors low enough whereas the probed objects are more and more difficult to handle when they scale down. Materials such as epoxy-based materials [1, 2], pure metals [3] and ceramics [4] have been shown to display such size-dependent elasticity. On the other hand, surface couplings at the micrometer-scale have been shown to be rather easy to implement since the mid 90s [5], and this triggered the development of micromechanical sensors [6]. Such developments clearly call for some dedicated frameworks to describe such scale effects for solids, and it is worth noting that most of these experimental results have been obtained on one-dimensional objects, thus stressing the need for tractable beam theories able to render these scale effects. This also holds true for (large scale) beams made of architected materials [7, 8].

An extremely vast number of such beam models has already been proposed in the literature [9]. To the best of the author's knowledge, they all fall into

two categories. Most of them, forming the first category, follow from the developments by Gurtin and Murdoch [10, 11] : the surface is considered as a membrane material withstanding “surface stresses” with its own mechanical properties , the membrane eigenstrain (and thus the surface energy) being possibly discarded. Such an approach has been shown to efficiently render size-dependent elasticity [3] and the thermodynamics of the involved chemical system can be used to set the properties of the surface when dealing with surface couplings [12, 13, 14] (also see [15] in the context of capillary actions). The question of the connection between both the properties and the mechanical state of the bulk and surface materials remains open, making the role of the material itself in the observed effects somehow unclear.

The second category gathers models which rely on different types of non-local formulations of the driving equations. Strongly non-local formulations [16] appear as the introduction of regularization operators whose physical meaning is sometimes questionable [17]. Alternatively, weakly non-local formulations rely on generalized continua, among which higher-grade continua feature a lower complexity, and as such have been preferentially considered to build simplified theories describing the behavior of one-dimensional objects. The constitutive equations then make coefficients scaling as stiffnesses multiplied by characteristic lengths to the various powers appear : first-strain gradient (FSG) elasticity [18] thus naturally renders size-dependent elasticity, whereas second-strain gradient (SSG) elasticity further introduces a cohesion modulus which has been shown to rigorously define the equivalent of surface tension for solids [19]. Interestingly, modeling surface tension effects in solids has recently (and rather independently) become an issue in the soft matter

community together with the definition of a cut-off length able to smooth stress singularities [20]. Several contributions focused on the assessment of the equivalence between membrane-based descriptions and higher-grade elasticity [21, 22]. These frameworks are thus particularly suited to describe scale effects in elasticity [23, 24], so that some efforts have been made to translate them to one-dimensional structures.

Focusing on beams, the vast majority of these attempts actually starts from one-dimensional analogues of the three-dimensional equations describing the continua [21, 25, 26, 27, 28, 29, 30]. This allows to introduce simplifications and adjust the complexity to the effects the authors wish to describe, but the link to the parameters in the three-dimensional constitutive laws is lost and so for the underlying thermodynamics, so that paradoxes may appear when comparing formulations [31, 32]. An alternative approach in such a complex situation consists in starting from the three-dimensional constitutive law to derive the beam equations. Even though the number of material parameters is rather large (18 elastic parameters are for instance necessary to describe an isotropic centrosymmetric material in SSG elasticity), the complexity is then kept reasonable by making a direct use of the three-dimensional constitutive law : the (higher-order) stresses in the beam are assumed to be obtained by applying it to the (higher-order) strain fields derived from the chosen beam kinematics [33, 34]. Static admissibility conditions are discarded, so that the resulting beam equations are shown to inherit some deficiencies from this construction, such as their inability to render Poisson's effect and the right tensile stiffness without a somehow arbitrary stiffness correction [33, 35]. This holds also true when simplified constitutive laws [36] are considered

[37]. Because the constitutive equations under scrutiny herein are too complex to allow for a direct asymptotic analysis [38], an alternative route has to be found, but the quantitative character of the available beam theories thus seems limited by the trade-off between complexity and thermodynamic groundings.

This contribution therefore intends to overcome this difficulty by proposing an approach to build beam equations for materials featuring higher-grade elasticity. It is aimed to include the static admissibility conditions, which are derived in Sect.(2) and which are missing in the above-mentioned approaches. The complexity is kept rather simple by making use of the constitutive equation gap [39] in Sect.(3). This approach is then applied to SSG elasticity in Sect.(4), for which all the involved terms are expressed as closed-forms and a variational formulation is derived. The resulting equations are finally solved for tensile and bending loadings in Sect.(5) in order to assess the role of the different grades and provide a base for the experimental identifiability of the constitutive parameters. The reader interested in applying these constitutively optimal governing equations to its own problem may directly jump to this Sect. and Appendix B for the closed-form expressions of the involved coefficients.

2. Problem statement

2.1. Geometry and kinematics

Considering a beam lying along \mathbf{x} direction and using the Euler-Bernoulli assumption, the displacement \mathbf{d} for a plane loading in the (\mathbf{x}, \mathbf{y}) plane reads

$$d_x = u(x) - y \frac{dv(x)}{dx} \quad (1)$$

$$d_y = v(x) \quad (2)$$

Following Mindlin [19], the free energy is assumed to depend on the classical infinitesimal strain ϵ^1 , as well as on the triadic $\epsilon^2 = \nabla \nabla \mathbf{d}$ (symmetric in the first two positions) and on $\epsilon^3 = \nabla \nabla \nabla \mathbf{d}$ (symmetric in the first three positions). ϵ^1 has therefore a single non-vanishing component

$$\epsilon_{xx} = -y \frac{d^2v}{dx^2} + \frac{du}{dx} \quad (3)$$

The non-zero components of ϵ^2 read

$$\epsilon_{xxx} = -y \frac{d^3v}{dx^3} + \frac{d^2u}{dx^2} \quad (4)$$

$$\epsilon_{xyx} = -\frac{d^2v}{dx^2} = \epsilon_{yxx} \quad (5)$$

$$\epsilon_{xxy} = \frac{d^2v}{dx^2} \quad (6)$$

The components of ϵ^3 read

$$\epsilon_{xxxx} = -y \frac{d^4v}{dx^4} + \frac{d^3u}{dx^3} \quad (7)$$

$$\epsilon_{yxxx} = -\frac{d^3v}{dx^3} = \epsilon_{xyxx} = \epsilon_{xxyx} \quad (8)$$

$$\epsilon_{xxxy} = \frac{d^3v}{dx^3} \quad (9)$$

2.2. Second-strain gradient elasticity

Let us assume that all the material parameters are uniform all over the cantilever beam. The approach proposed herein will be illustrated throughout the manuscript considering the second-strain gradient elasticity (SSG) of a centrosymmetric, isotropic material [19]. The free energy density ψ therefore reads

$$\begin{aligned}
\psi = & \frac{\lambda}{2}\epsilon_{ii}\epsilon_{jj} + \mu\epsilon_{ij}\epsilon_{ij} \\
& + a_1\epsilon_{ijj}\epsilon_{ikk} + a_2\epsilon_{iik}\epsilon_{kjj} + a_3\epsilon_{iik}\epsilon_{jjk} + a_4\epsilon_{ijk}\epsilon_{ijk} + a_5\epsilon_{ijk}\epsilon_{kji} \\
& + b_1\epsilon_{iij}\epsilon_{kkll} + b_2\epsilon_{ijkk}\epsilon_{ijll} + b_3\epsilon_{iijk}\epsilon_{jkl} + b_4\epsilon_{iijk}\epsilon_{llkj} \\
& + b_5\epsilon_{iijk}\epsilon_{lljk} + b_6\epsilon_{ijkl}\epsilon_{ijkl} + b_7\epsilon_{ijkl}\epsilon_{jkli} \\
& + c_1\epsilon_{ii}\epsilon_{jjkk} + c_2\epsilon_{ij}\epsilon_{ijkk} + c_3\epsilon_{ij}\epsilon_{kkij} \\
& + b_0\epsilon_{iijj}
\end{aligned} \tag{10}$$

where λ and μ are Lamé's coefficients, whereas the other parameters

$$\begin{aligned}
a_n, c_n, b_0 & \propto \mu l_S^2 \\
b_n & \propto \mu l_S^4
\end{aligned}$$

make characteristic lengths $\propto l_S$ appear. The presence of the linear term proportional to ϵ_{iijj} is to be highlighted. Without any external loading, it makes the free energy non-zero

$$\psi = \frac{b_0}{2}\Delta(\operatorname{div}\mathbf{u})$$

and b_0 , which is denoted as the cohesion modulus, defines the equivalent of surface tension for solids [19]. Defining the associated generalized stresses as

$$\begin{aligned}\tau^1 &= \frac{\partial\psi}{\partial\epsilon^1} \\ \tau^2 &= \frac{\partial\psi}{\partial\epsilon^2} \\ \tau^3 &= \frac{\partial\psi}{\partial\epsilon^3}\end{aligned}\tag{11}$$

, the virtual work principle reads, $\forall d^*$ (admissible)

$$\int_V W(d^*)dV = \int_V (\tau^1 : \epsilon^1(d^*) + \tau^2 : \epsilon^2(d^*) + \tau^3 : \epsilon^3(d^*)) dV = \mathcal{W}_{ext}(d^*)\tag{12}$$

Restricting to the derivation of beam equations, d^* derives from the chosen kinematics (Euler-Bernoulli, Timoshenko...). τ^i and ϵ^i are not necessarily associated through Eqs.(10) and (11), so that a choice has to be made. As already outlined in the introduction, the literature assumes, for the sake simplicity, that τ^i and ϵ^i are associated through the 3D laws, so that the equations recalled in Appendix A hold [33, 34]. It should actually be highlighted that the usual (Cauchy) elastic beam theories make use of $\sigma_{xx} = E\epsilon_{xx}$ at the local scale, where E is the Young's modulus, which differs from the coefficient $\lambda + 2\mu$ obtained from the three-dimensional law. It is well known this difference arises from the static boundary conditions. The purpose of the next sections is thus to define the static admissibility conditions which have been discarded so far and which should be taken into account to correct such a deficiency.

2.3. Static boundary conditions

Denoting

$$\mathbf{n} = \begin{bmatrix} 0 \\ \cos \alpha \\ \sin \alpha \end{bmatrix} \quad (13)$$

the normal at the cross-section boundary, one assumes, for classical beam theories, that the tractions at any beam boundary vanish :

$$\tau^1 \mathbf{n} = \mathbf{0} \quad \forall \alpha \quad (14)$$

which is imposed by simultaneously ensuring

$$\mathbf{y}^t \tau^1 \mathbf{n} = 0 \quad \forall \alpha \quad (15)$$

$$\mathbf{z}^t \tau^1 \mathbf{n} = 0 \quad \forall \alpha \quad (16)$$

$$\mathbf{x}^t \tau^1 \mathbf{n} = 0 \quad \forall \alpha \quad (17)$$

Eqs. (15-16) are usually ensured by setting (using the symmetry of τ^1) :

$$\tau_{yy} = \tau_{zz} = \tau_{yz} = 0 \quad (18)$$

for all points P within the cross-section \mathcal{S} , whereas Eq.(17) has to be satisfied at the boundary \mathcal{B} . This set of conditions defines the statically admissible stress fields when using Cauchy elasticity. This section intends to extend such approach to second strain gradient elasticity.

2.3.1. Third-order traction

The general form of boundary conditions is given in [19], Eq.(18). Eq. (18c) reads (using symmetry relationships):

$$\begin{aligned} \mathbf{t}^3 = & \cos^3 \alpha \begin{bmatrix} \tau_{yyyyx} \\ \tau_{yyyyy} \\ \tau_{yyyzy} \end{bmatrix} + 3 \cos^2 \alpha \sin \alpha \begin{bmatrix} \tau_{yyzx} \\ \tau_{yyzy} \\ \tau_{yyzz} \end{bmatrix} + 3 \cos \alpha \sin^2 \alpha \begin{bmatrix} \tau_{yzzx} \\ \tau_{yzzzy} \\ \tau_{yzzzz} \end{bmatrix} \\ & + \sin^3 \alpha \begin{bmatrix} \tau_{zzzx} \\ \tau_{zzzy} \\ \tau_{zzzz} \end{bmatrix} \end{aligned} \quad (19)$$

Similarly imposing $\mathbf{y} \cdot \mathbf{t}^3 = 0 \forall \alpha$ and $\mathbf{z} \cdot \mathbf{t}^3 = 0 \forall \alpha$ for all points within the beam cross-section yields

$$\mathcal{H}_{3s} : \begin{cases} \tau_{yyyy} = \tau_{yyzy} = \tau_{yzzzy} = \tau_{zzzy} = 0 \\ \tau_{yyyzy} = \tau_{yyzzz} = \tau_{yzzzz} = \tau_{zzzz} = 0 \end{cases} \quad \forall P \in \mathcal{S} \quad (20)$$

Further imposing $\mathbf{x} \cdot \mathbf{t}^3 = 0 \forall \alpha$ at the boundary yields

$$\mathcal{H}_{3b} : 0 = \cos^3 \alpha \tau_{yyyx} + 3 \cos^2 \alpha \sin \alpha \tau_{yyzx} + 3 \cos \alpha \sin^2 \alpha \tau_{yzzx} + \sin^3 \alpha \tau_{zzzx} \quad \forall \alpha \forall P \in \mathcal{B} \quad (21)$$

2.3.2. Second-order traction

Expanding Mindlin's \mathbf{L} operator, Eq. (18b) in [19] reads (using symmetry relationships)

$$\mathbf{t}^2 = \mathbf{nn} : (\tau^2 - \nabla \cdot \tau^3) + 2(\overset{s}{\nabla} \cdot \mathbf{n})\mathbf{t}^3 - \mathbf{n} \cdot \left[\overset{s}{\nabla} \cdot (\mathbf{n} \cdot \tau^3) \right] - \overset{s}{\nabla} \cdot (\mathbf{nn} : \tau^3) \quad (22)$$

One thus has to satisfy, for all points of the cross-section :

$$\mathbf{y} \cdot \mathbf{t}^2 = 0 \quad \forall \alpha \quad (23)$$

$$\mathbf{z} \cdot \mathbf{t}^2 = 0 \quad \forall \alpha \quad (24)$$

where \mathbf{t}^2 expands as

$$\begin{aligned}
\mathbf{t}^2 &= 2(\overset{s}{\nabla} \cdot \mathbf{n})\mathbf{t}^3 \\
&\quad -2 \cos^4 \alpha \tau_{yyzk,z} - 2 \sin^4 \alpha \tau_{yzzk,y} \\
&\quad +2 \cos^3 \alpha \sin \alpha (\tau_{yyyk,z} + \tau_{yyzk,y} - 2\tau_{yzzk,z}) \\
&\quad -2 \cos^2 \alpha \sin^2 \alpha (\tau_{yyyk,y} - 2\tau_{yyzk,z} - 2\tau_{yzzk,y} + \tau_{zzzk,z}) \\
&\quad -2 \cos \alpha \sin^3 \alpha (2\tau_{yyzk,y} - \tau_{yzzk,z} - \tau_{zzzk,y}) \\
&\quad + \cos^2 \alpha (\tau_{yyk} - \tau_{lyyk,l} - 2\tau_{xyyk,x}) \\
&\quad +2 \cos \alpha \sin \alpha (\tau_{yzk} - \tau_{lyzk,l} - 2\tau_{xyzk,x}) \\
&\quad + \sin^2 \alpha (\tau_{zzk} - \tau_{lzzk,l} - 2\tau_{xzzk,x}) \\
&\quad +3f_c (\cos^2 \alpha \tau_{yyzk} + \cos \alpha \sin \alpha (\tau_{yzzk} - \tau_{yyyk}) - \sin^2 \alpha \tau_{yyzk}) \\
&\quad +3f_s (\cos^2 \alpha \tau_{yzzk} + \cos \alpha \sin \alpha (\tau_{zzzk} - \tau_{yyzk}) - \sin^2 \alpha \tau_{yzzk}) \quad (25)
\end{aligned}$$

with

$$f_c = \sin \alpha \frac{\partial \cos \alpha}{\partial y} - \cos \alpha \frac{\partial \cos \alpha}{\partial z} \quad (26)$$

$$f_s = \sin \alpha \frac{\partial \sin \alpha}{\partial y} - \cos \alpha \frac{\partial \sin \alpha}{\partial z} \quad (27)$$

Assuming that the condition \mathcal{H}_{3s} is satisfied, Eqs.(23-24) yield :

$$\mathcal{H}_{2s} : \begin{cases} \tau_{yyk} = 3 \tau_{xyyk,x} \\ \tau_{yzk} = 3 \tau_{xyzk,x} \\ \tau_{zzk} = 3 \tau_{xzzk,x} \end{cases} \quad \forall P \in \mathcal{S}, k = y \text{ or } k = z \quad (28)$$

The condition $\mathbf{x} \cdot \mathbf{t}^2 = 0 \quad \forall \alpha \quad \forall P \in \mathcal{B}$ has also to be satisfied, and has to be examined for any particular loading and geometry.

2.3.3. First-order traction

Expanding the \mathbf{L} operator, Eq. (18c) in [19] reads (using symmetry relationships)

$$\begin{aligned} \mathbf{t}^1 = & \mathbf{n} \cdot (\tau^1 - \nabla \cdot \tau^2 + \nabla \nabla : \tau^3) + (\overset{s}{\nabla} \cdot \mathbf{n}) \left[\mathbf{t}^2 - (\overset{s}{\nabla} \cdot \mathbf{n}) \mathbf{t}^3 \right] \\ & - \overset{s}{\nabla} \cdot \left[\mathbf{n} \cdot (\tau^2 - \nabla \cdot \tau^3) - \overset{s}{\nabla} \cdot (\mathbf{n} \cdot \tau^3) - (\overset{s}{\nabla} \mathbf{n}) \cdot (\mathbf{nn} : \tau^3) \right] \end{aligned} \quad (29)$$

Imposing, at any point of the cross-section

$$\mathbf{y} \cdot \mathbf{t}^1 = 0 \quad \forall \alpha \quad (30)$$

$$\mathbf{z} \cdot \mathbf{t}^1 = 0 \quad \forall \alpha \quad (31)$$

yields, assuming that both \mathcal{H}_{3s} and \mathcal{H}_{2s} are satisfied :

$$\mathcal{H}_{1s} : \begin{cases} \tau_{yk} - 2 \tau_{xyk,x} + 3 \tau_{xxyk,xx} = 0 \\ \tau_{zk} - 2 \tau_{xzk,x} + 3 \tau_{xxzk,xx} = 0 \end{cases} \quad \forall P \in \mathcal{S}, k = y \text{ or } k = z \quad (32)$$

Similarly, the condition $\mathbf{x} \cdot \mathbf{t}^1 = 0 \quad \forall \alpha \quad \forall P \in \mathcal{B}$ should be examined for the considered loading and geometry.

2.4. Statically admissible (higher-order) stress fields

Extending the approach used for classical beam theories, one defines the statically admissible (higher-order) stress fields as those simultaneously satisfying conditions \mathcal{H}_{3s} , \mathcal{H}_{2s} and \mathcal{H}_{1s} . This set of conditions thus defines a space of statically admissible stress fields Θ . The vector \mathbf{T} gathers the

involved stress components :

$$\begin{aligned}
\mathbf{T}^t = & \left[\tau_{xx}, \tau_{yy}, \tau_{zz}, \sqrt{2}\tau_{yz}, \sqrt{2}\tau_{xz}, \sqrt{2}\tau_{xy}, \right. \\
& \tau_{xxx}, \tau_{yyx}, \tau_{zzx}, \sqrt{2}\tau_{yzx}, \sqrt{2}\tau_{xzx}, \sqrt{2}\tau_{xyx}, \\
& \tau_{xxy}, \tau_{yyy}, \tau_{zzy}, \sqrt{2}\tau_{yzy}, \sqrt{2}\tau_{xzy}, \sqrt{2}\tau_{xyy}, \\
& \tau_{xxz}, \tau_{yyz}, \tau_{zzz}, \sqrt{2}\tau_{yzz}, \sqrt{2}\tau_{xzz}, \sqrt{2}\tau_{xyz}, \\
& \tau_{xxxx}, \tau_{yyyy}, \tau_{zzzx}, \sqrt{3}\tau_{yzzx}, \sqrt{3}\tau_{yyzx}, \sqrt{6}\tau_{xyzx}, \sqrt{3}\tau_{xzzx}, \sqrt{3}\tau_{xxzx}, \sqrt{3}\tau_{xxyx}, \sqrt{3}\tau_{xyyx}, \\
& \tau_{xxxy}, \tau_{yyyy}, \tau_{zzzy}, \sqrt{3}\tau_{yzzzy}, \sqrt{3}\tau_{yyzy}, \sqrt{6}\tau_{xyzzy}, \sqrt{3}\tau_{xzzzy}, \sqrt{3}\tau_{xxzy}, \sqrt{3}\tau_{xxyy}, \sqrt{3}\tau_{xyyy}, \\
& \left. \tau_{xxxz}, \tau_{yyyz}, \tau_{zzzz}, \sqrt{3}\tau_{yzzz}, \sqrt{3}\tau_{yyzz}, \sqrt{6}\tau_{xyzzz}, \sqrt{3}\tau_{xzzz}, \sqrt{3}\tau_{xxzz}, \sqrt{3}\tau_{xxyz}, \sqrt{3}\tau_{xyyz} \right]
\end{aligned} \tag{33}$$

so that

$$\Theta : \{\mathbf{T}/\mathcal{H}_{1s}\} \cap \{\mathbf{T}/\mathcal{H}_{2s}\} \cap \{\mathbf{T}/\mathcal{H}_{3s}\} \tag{34}$$

The stresses resulting from an Euler-Bernoulli displacement field through the three-dimensional constitutive law are detailed in Appendix A (see Eqs. A.8-A.24). It is straightforward to note that these stresses do not belong to the Θ subspace. There exists a gap between the stresses obtained from the displacement field and those belonging to the admissible space Θ . A direct comparison of the conditions \mathcal{H}_{3s} , \mathcal{H}_{2s} and \mathcal{H}_{1s} with the stress values obtained from the three-dimensional constitutive law thus brings to the conclusion that all conditions (Euler-Bernoulli kinematics, three-dimensional constitutive law and free-boundaries conditions) cannot be met simultaneously, and one has to somehow relax the constrains.

3. Optimal constitutive equations for beams

It is actually proposed to make the constitutive equation accommodate both the kinematic and free-boundaries conditions. As the static and kinematic fields cannot be related through the three-dimensional constitutive law, the latter has to be replaced. The challenge is then to rigorously define the constitutive law to be used when writing the virtual work principle (12) instead of the three-dimensional law. This Section details the use of the so-called constitutive equation gap [39] for that purpose.

3.1. Constitutive equation gap

The free energy density ψ formally reads (see Eq.(10))

$$\psi(\mathbf{E}) = \frac{1}{2}\mathbf{E} \cdot \mathcal{C} \cdot \mathbf{E} + \mathbf{B} \cdot \mathbf{E} \quad (35)$$

where \mathbf{E} is the vector gathering the kinematic variables :

$$\begin{aligned} \mathbf{E}^t = & \left[\begin{array}{l} \epsilon_{xx}, \epsilon_{yy}, \epsilon_{zz}, \sqrt{2}\epsilon_{yz}, \sqrt{2}\epsilon_{xz}, \sqrt{2}\epsilon_{xy}, \\ \epsilon_{xxx}, \epsilon_{yyx}, \epsilon_{zzx}, \sqrt{2}\epsilon_{yzx}, \sqrt{2}\epsilon_{xxz}, \sqrt{2}\epsilon_{xyx}, \\ \epsilon_{xxy}, \epsilon_{yyy}, \epsilon_{zzy}, \sqrt{2}\epsilon_{yzy}, \sqrt{2}\epsilon_{xzy}, \sqrt{2}\epsilon_{xyy}, \\ \epsilon_{xxz}, \epsilon_{yyz}, \epsilon_{zzz}, \sqrt{2}\epsilon_{yzz}, \sqrt{2}\epsilon_{xzz}, \sqrt{2}\epsilon_{xyz}, \\ \epsilon_{xxxx}, \epsilon_{yyyx}, \epsilon_{zzzx}, \sqrt{3}\epsilon_{yzzx}, \sqrt{3}\epsilon_{yyzx}, \sqrt{6}\epsilon_{xyzx}, \sqrt{3}\epsilon_{xzzx}, \sqrt{3}\epsilon_{xxzx}, \sqrt{3}\epsilon_{xxyx}, \sqrt{3}\epsilon_{xyyx}, \\ \epsilon_{xxxy}, \epsilon_{yyyy}, \epsilon_{zzzy}, \sqrt{3}\epsilon_{yzzzy}, \sqrt{3}\epsilon_{yyzy}, \sqrt{6}\epsilon_{xyzy}, \sqrt{3}\epsilon_{xzzzy}, \sqrt{3}\epsilon_{xxzy}, \sqrt{3}\epsilon_{xxyy}, \sqrt{3}\epsilon_{xyyy}, \\ \epsilon_{xxxz}, \epsilon_{yyyz}, \epsilon_{zzzz}, \sqrt{3}\epsilon_{yzzz}, \sqrt{3}\epsilon_{yyzz}, \sqrt{6}\epsilon_{xyzz}, \sqrt{3}\epsilon_{xzzz}, \sqrt{3}\epsilon_{xxzz}, \sqrt{3}\epsilon_{xxyz}, \sqrt{3}\epsilon_{xyyz} \end{array} \right] \end{aligned} \quad (36)$$

of kinematically admissible fields :

$$\Xi = \left\{ \mathbf{E}^t = \left[\begin{array}{l} \epsilon_{xx}, 0, 0, 0, 0, 0, \frac{\partial \epsilon_{xx}}{\partial x}, 0, 0, 0, 0, \sqrt{2} \frac{\partial \epsilon_{xx}}{\partial y}, -\frac{\partial \epsilon_{xx}}{\partial y}, 0, 0, 0, 0, 0, \\ 0, 0, 0, 0, 0, 0, \frac{\partial^2 \epsilon_{xx}}{\partial x^2}, 0, 0, 0, 0, 0, 0, \sqrt{3} \frac{\partial^2 \epsilon_{xx}}{\partial x \partial y}, 0, -\frac{\partial^2 \epsilon_{xx}}{\partial x \partial y}, 0, \\ 0, 0, 0, 0, 0, 0, 0, 0, 0, 0, 0, 0, 0, 0, 0, 0 \end{array} \right], \epsilon_{xx} = -y \frac{d^2 v}{dx^2} + \frac{du}{dx} \right\} \quad (41)$$

As recalled in Sect.2.2, it is usually chosen in Eq.(12) [33, 34] to set $W(\mathbf{d}^*)$ as

$$\begin{aligned} W(\mathbf{d}^*) &= (\mathbf{C} \cdot \mathbf{E}_{KA} + \mathbf{B}) \cdot \mathbf{E}(\mathbf{d}^*) \\ \mathbf{E}_{KA} &\in \Xi \\ \mathbf{E}(\mathbf{d}^*) &\in \Xi \end{aligned} \quad (42)$$

thus assuming the three-dimensional constitutive law is satisfied, without any consideration for any (free) boundary condition. Such a choice is known to yield deficient governing equations :

- In the context of Cauchy elasticity, it is recalled in Appendix C that it results in an incorrect tensile stiffness and unbalanced stresses at the cross-section boundary, because the static admissibility conditions (and thus the Poisson effect) are not taken into account.
- In the context of second-strain gradient elasticity, this makes the governing equations converge towards equations exhibiting the same deficiencies. The longitudinal stiffness is then arbitrarily rescaled to match the Young's modulus when the beam dimensions are large enough, but this choice is definitely not unique and lacks a justification [33, 34].

The key to fix these deficiencies is to account for the static admissibility conditions, and the challenge is to keep it rather simple, even for complicated constitutive equations. It is thus suggested to replace Eq.(42) by

$$\begin{aligned}
W(\mathbf{d}^*) &= \mathbf{T}_{SA} \cdot \mathbf{E}(\mathbf{d}^*) \\
\mathbf{T}_{SA} &= \text{Arg min}_{\mathbf{T} \in \Theta} \eta_\psi(\mathbf{T}, \mathbf{E}_{KA}) \\
\mathbf{E}_{KA} &\in \Xi \\
\mathbf{E}(\mathbf{d}^*) &\in \Xi
\end{aligned} \tag{43}$$

\mathbf{T}_{SA} is thus the statically admissible stress state satisfying at best the three-dimensional constitutive law for Euler-Bernoulli displacement fields. The constitutive equation gap has been initially proposed to assess the quality of finite-element analysis by measuring the distance between statically admissible fields and kinematically admissible ones [39]. It is proposed herein to use it to define the constitutive equations making the kinematically admissible and statically admissible fields correspond, while keeping the “distance” to the three-dimensional constitutive law minimal in the sense of the chosen norm. Such constitutive equations are denoted as optimal is the following.

3.2. Optimal constitutive equations

$\eta_\psi(\mathbf{T}, \mathbf{E}_{KA})$ is a quadratic function of the stress components, so that the minimizer \mathbf{T}_{SA} is defined by a set of linear equations obtained by expressing the stationarity of $\eta_\psi(\mathbf{T}, \mathbf{E}_{KA})$ with respect to the components of $\mathbf{T} \in \Theta$. This latter condition is enforced by setting

$$\mathbf{T} = \mathcal{P}_\Theta \mathbf{T}_\Theta \tag{44}$$

where \mathbf{T}_Θ is the vector

$$\begin{aligned}
\mathbf{T}_\Theta^t = & \left[\tau_{xx}, \tau_{xz}, \tau_{xy}, \tau_{xxx}, \tau_{yyx}, \tau_{zzx}, \tau_{yza}, \tau_{xxa}, \tau_{xya}, \right. \\
& \tau_{xxy}, \tau_{xzy}, \tau_{xyy}, \tau_{axz}, \tau_{axz}, \tau_{xyz}, \\
& \tau_{xxx}, \tau_{yyy}, \tau_{zzz}, \tau_{yzz}, \tau_{yyz}, \tau_{xyza}, \tau_{axza}, \tau_{axza}, \tau_{xxya}, \tau_{xyya}, \\
& \tau_{xxy}, \tau_{xyzy}, \tau_{axzy}, \tau_{xxyy}, \tau_{xyyy}, \tau_{axxz}, \tau_{xyzz}, \tau_{axzz}, \tau_{xxyz}, \tau_{xyyz}, \\
& \left. \tau_{xyy,x}, \tau_{axz,x}, \tau_{xyy,x}, \tau_{xyzy,x}, \tau_{axzy,x}, \tau_{xyyy,x}, \tau_{xyzz,x}, \tau_{axzz,x}, \tau_{xyyz,x}, \tau_{xxyy,xx}, \tau_{axzz,xx}, \tau_{xyyz,xx} \right]
\end{aligned} \tag{45}$$

and \mathcal{P}_Θ is the 54×49 operator defined from the conditions (20), (28) and (32). The stationarity of $\eta_\psi(\mathcal{P}_\Theta \mathbf{T}_\Theta, \mathbf{E}_{KA})$ with respect to the components of \mathbf{T}_Θ thus defines the optimal $\hat{\mathbf{T}}_\Theta$

$$(\mathcal{P}_\Theta^t \mathcal{C}^{-1} \mathcal{P}_\Theta) \hat{\mathbf{T}}_\Theta = \mathcal{P}_\Theta^t (\mathbf{E}_{KA} + \mathcal{C}^{-1} \mathbf{B}) \tag{46}$$

The procedure to easily solve Eq. (46) is detailed in Appendix B. The resulting constitutive equations are formally denoted as

$$\mathbf{T}_{SA} = \mathcal{C}_{opt}^{EB} \mathbf{E}_{KA} + \mathbf{B}_{opt}^{EB} \tag{47}$$

The detailed expressions of the optimal constitutive law are also given in Appendix B, and the local constitutive equation gap $\eta_\psi(\mathcal{C}_{opt}^{EB} \mathbf{E}_{KA} + \mathbf{B}_{opt}^{EB}, \mathbf{E}_{KA}) > 0$ may be expressed as a function of the local kinematic variables. The same construction is detailed for Cauchy materials in Appendix C and is shown to yield the classical beam equations.

4. Application to second-strain gradient elasticity

The expression of the \mathbf{T}_{SA} components have been obtained as closed forms in Appendix B for second-strain gradient elasticity. It should be outlined

that these closed forms have been obtained using the general constitutive law as formulated by Mindlin [19], so that simplified forms resulting from specific choices of the constitutive parameters [36, 37, 40, 41] can easily be derived. Similarly to the residual constitutive equation gap analysis provided in Appendix C, it can be shown that the remaining error is solely located on (higher-order) strain components within the cross-section plane, so that the other components may be considered as accurate.

4.1. Comparison to 3D law for stresses involved in Euler-Bernoulli equations

The differences with stresses obtained when discarding the static admissibility conditions (see Appendix A) are now examined. Focusing on the derivation of an Euler-Bernoulli beam theory with a uniform cohesion modulus, the optimal stresses τ_{xx} , τ_{xxx} , τ_{xyx} , τ_{xxy} , τ_{xxxx} , τ_{xxyx} and τ_{xxxy} above should be compared to their 3D counterpart summarized in Appendix A.

$$\begin{aligned} \tau_{xx} = & C_{xx}^{xx}\epsilon_{xx} + C_{xx}^{xxxx}\epsilon_{xxxx} + C_{xx}^0 b_0 \\ & + C_{xx}^{ix} \left(e^{\alpha\gamma x} \int^x \epsilon_{xxxx}(\eta) e^{-\alpha\gamma\eta} d\eta - e^{-\alpha\gamma x} \int^x \epsilon_{xxxx}(\eta) e^{\alpha\gamma\eta} d\eta \right) \end{aligned} \quad (48)$$

$$\tau_{xxx} = C_{xxx}^{xxx}\epsilon_{xxx} = 2(a_1 + a_2 + a_3 + a_4 + a_5)\epsilon_{xxx} \quad (49)$$

$$\tau_{xyx} = C_{xyx}^{xxy}\epsilon_{xxy} + C_{xyx}^{xxxxxy} \frac{\partial \epsilon_{xxxxy}}{\partial x} \quad (50)$$

$$\tau_{xxy} = C_{xxy}^{xxy}\epsilon_{xxy} + C_{xxy}^{xxxxxy} \frac{\partial \epsilon_{xxxxy}}{\partial x} \quad (51)$$

$$\begin{aligned} \tau_{xxxx} = & C_{xxxx}^{xx}\epsilon_{xx} + C_{xxxx}^{xxxx}\epsilon_{xxxx} + C_{xxxx}^0 b_0 \\ & + C_{xxxx}^{ix} \left(e^{\alpha\gamma x} \int^x \epsilon_{xxxx}(\eta) e^{-\alpha\gamma\eta} d\eta - e^{-\alpha\gamma x} \int^x \epsilon_{xxxx}(\eta) e^{\alpha\gamma\eta} d\eta \right) \end{aligned} \quad (52)$$

$$\tau_{xxyx} = C_{xxyx}^{xxxxy}\epsilon_{xxxxy} = -\frac{1}{3}(4b_2 + b_3 - 2b_4 + 2b_5 + 6b_6 + 2b_7)\epsilon_{xxxxy} \quad (53)$$

$$\tau_{xxxy} = C_{xxxy}^{xxxxy}\epsilon_{xxxxy} = -(b_3 + 2b_4 - 2b_5 - 2b_6 + 2b_7)\epsilon_{xxxxy} \quad (54)$$

α_7 results from the material parameters and is defined as

$$\alpha_7^2 = \frac{2((\lambda + \mu)(3b_7 + 3b_6 + 4b_5 + 4b_4 + 4b_3 + 4b_2 + 8b_1) - (c_3 + c_2 + 2c_1)^2)}{(c_3 + 2c_1)(3b_7 + 3b_6 + 2b_3 + 4b_2) - c_2(4b_5 + 4b_4 + 2b_3 + 8b_1)} \quad (55)$$

As the Euler-Bernoulli kinematic assumptions impose that $\epsilon_{xxyx} = -\epsilon_{xxxy}$, it should first be noticed that τ_{xxx} , τ_{xxyx} and τ_{xxxy} remain unchanged by the optimization procedure. Contrarily, τ_{xyx} and τ_{xxy} now also depend on the local variations on the (higher-order) strain field. Changes in the beam equations are thus to be expected. τ_{xxxx} is significantly modified by an additional, non-local term depending on the higher-order strains. τ_{xx} is also altered by a similar non-local term. It should be emphasized that these non-local terms result from the optimization procedure. The exponential weight function results from the differential constraints and the characteristic length α_7^{-1} now results from the constitutive parameters (Eq.(55)) instead of being postulated as for Eringen-like elasticity [16].

τ_{xx} and τ_{xxxx} are furthermore modified by a new term proportional to the cohesion modulus, which directly results from the optimality conditions. The beam equations describing a chemical surface modification are thus expected to be greatly modified by this direct contribution of the cohesion modulus to the Cauchy stress tensor, which is absent from the equations derived without consideration for the static admissibility conditions [33]. This direct coupling between the Cauchy stress and the surface energy through the cohesion modulus is a clear indication that the present approach paves the way to description of the chemo-mechanical couplings at stake in cantilever sensors. It should finally be outlined that these differences prove that the remaining constitutive equation gap $\min_{\mathbf{T} \in \Theta} \eta_\psi(\mathbf{T}, \mathbf{E}_{KA}) \neq 0$ in general.

4.2. Special case : First strain gradient

Setting the second strain-gradient components to zero still makes some higher-order stress components different from those deduced from the 3D law :

$$\tau_{xyx} = C_{xyx}^{xxy} \epsilon_{xxy} \quad (56)$$

$$\tau_{xxy} = C_{xxy}^{xxy} \epsilon_{xxy} \quad (57)$$

$$\tau_{xzz} = \frac{a_2 + 2a_1}{2} \epsilon_{xxx} \quad (58)$$

$$\tau_{yyx} = (a_2 + 2a_3) \epsilon_{xxx} = \tau_{zzx} \quad (59)$$

$$\tau_{yyy} = \tau_{zzy} = 0 \quad (60)$$

The coefficients C_{xyx}^{xxy} and C_{xxy}^{xxy} are such that the stresses τ_{xyx} and τ_{xxy} now differ from those resulting from the 3D constitutive law. The other stress components are left unmodified.

4.3. Special case : Cauchy materials

Setting $b_0 = 0$ and neglecting higher-order strains yields

$$\tau_{xx} = C_{xx}^{xx} \epsilon_{xx} \quad (61)$$

$$\tau_{xy} = 0 \quad (62)$$

$$\tau_{xz} = 0 \quad (63)$$

$$\tau_{yy} = 0 \quad (64)$$

$$\tau_{yz} = 0 = \tau_{zy} \quad (65)$$

$$(66)$$

In addition,

$$\lim_{c_i \rightarrow 0} C_{xx}^{xx} = \frac{\mu(3\lambda + 2\mu)}{(\lambda + \mu)} = E \quad (67)$$

so that the usual relations for Cauchy materials are recovered.

4.4. Virtual work principle for a beam featuring a uniform b_0

One considers in the following a cantilever beam (length L) with a rectangular cross-section (thickness t and width b). Assuming that b_0 is uniform

along the beam, the virtual work principle reads $\forall \mathbf{d}^*$:

$$\begin{aligned}
& b^{-1}t^{-1} \int_0^L \int_{-\frac{b}{2}}^{\frac{b}{2}} \int_{-\frac{t}{2}}^{\frac{t}{2}} W(\mathbf{d}^*) dy dz dx = \\
& - \int_0^L \left(C_{xxxx} \frac{d^6 u}{dx^6} + (C_{xxx} + C_{xxxx} - C_{xxx}) \frac{d^4 u}{dx^4} + C_{xx} \frac{d^2 u}{dx^2} + C_{ix} \frac{d \bar{I}_x}{dx} + C_{xxxx} \frac{d^3 \bar{I}_x}{dx^3} \right) u^*(x) dx \\
& + \left[u^*(x) \left(C_{xxxx} \frac{d^5 u}{dx^5} + (C_{xxx} + C_{xxxx} - C_{xxx}) \frac{d^3 u}{dx^3} + C_{xx} \frac{du}{dx} + C_{xx}^0 \bar{b}_0 + C_{ix} \bar{I}_x + C_{xxxx} \frac{d^2 \bar{I}_x}{dx^2} \right) \right]_0^L \\
& - \left[\frac{du^*(x)}{dx} \left(C_{xxxx} \frac{d^4 u}{dx^4} + (C_{xxx} - C_{xxx}) \frac{d^2 u}{dx^2} + C_{ix} \frac{d \bar{I}_x}{dx} \right) \right]_0^L \\
& + \left[\frac{d^2 u^*(x)}{dx^2} \left(C_{xxxx} \frac{d^3 u}{dx^3} + C_{xxx} \frac{du}{dx} + C_{xxxx}^0 \bar{b}_0 + C_{xxxx} \bar{I}_x \right) \right]_0^L \\
& + \int_0^L \left(\frac{C_{xxxx} t^2}{12} \frac{d^8 v}{dx^8} + \left(t^2 \frac{C_{xxx} + C_{xxxx} - C_{xxx}}{12} - 2C_{xyx} + C_{xyx} + 3C_{xyx} - C_{xyx} \right) \frac{d^6 v}{dx^6} \right. \\
& \quad \left. + \left(C_{xyx} - 2C_{xyx} + C_{xx} \frac{t^2}{12} \right) \frac{d^4 v}{dx^4} - t \left(C_{ix} \frac{d^4 \bar{I}_x}{dx^4} + C_{ix} \frac{d^2 \bar{I}_x}{dx^2} \right) \right) v^*(x) dx \\
& - \left[v^*(x) \left(\frac{C_{xxxx} t^2}{12} \frac{d^7 v}{dx^7} + \left(t^2 \frac{C_{xxx} + C_{xxxx} - C_{xxx}}{12} - 2C_{xyx} + C_{xyx} + 3C_{xyx} - C_{xyx} \right) \frac{d^5 v}{dx^5} \right. \right. \\
& \quad \left. \left. + \left(C_{xyx} - 2C_{xyx} + C_{xx} \frac{t^2}{12} \right) \frac{d^3 v}{dx^3} - t \left(C_{ix} \frac{d^3 \bar{I}_x}{dx^3} + C_{ix} \frac{d \bar{I}_x}{dx} \right) \right) \right]_0^L \\
& + \left[\frac{dv^*(x)}{dx} \left(\frac{C_{xxxx} t^2}{12} \frac{d^6 v}{dx^6} + \left(C_{xyx} - 2C_{xyx} + C_{xx} \frac{t^2}{12} \right) \frac{d^2 v}{dx^2} - t \left(C_{ix} \frac{d^2 \bar{I}_x}{dx^2} + C_{ix} \bar{I}_x \right) \right. \right. \\
& \quad \left. \left. + \left(t^2 \frac{C_{xxx} + C_{xxxx} - C_{xxx}}{12} - 2C_{xyx} + C_{xyx} + 3C_{xyx} - C_{xyx} \right) \frac{d^4 v}{dx^4} \right) \right]_0^L \\
& - \left[\frac{d^2 v^*(x)}{dx^2} \left(\frac{C_{xxxx} t^2}{12} \frac{d^5 v}{dx^5} + \left(t^2 \frac{C_{xxx} - C_{xxx}}{12} + 3C_{xyx} - C_{xyx} \right) \frac{d^3 v}{dx^3} - t C_{ix} \frac{d \bar{I}_x}{dx} \right) \right]_0^L \\
& + t \left[\frac{d^3 v^*(x)}{dx^3} \left(\frac{C_{xxxx} t}{12} \frac{d^4 v}{dx^4} + \frac{C_{xxx} t}{12} \frac{d^2 v}{dx^2} - C_{ix} \bar{I}_x \right) \right]_0^L \tag{68}
\end{aligned}$$

where

$$\int_{-\frac{t}{2}}^{\frac{t}{2}} b_0(y) dy = t \bar{b}_0 \tag{69}$$

It should first be noticed that the tension and bending problems are decoupled, as for Cauchy elasticity. Two differences are to be highlighted in comparison to the variational principles derived from the 3D constitutive laws (see [33]) :

- Every term is altered by

$$I_x = e^{\alpha_7 x} \int^x \epsilon_{xxxx}(\eta) e^{-\alpha_7 \eta} d\eta - e^{-\alpha_7 x} \int^x \epsilon_{xxxx}(\eta) e^{\alpha_7 \eta} d\eta \quad (70)$$

or one of its derivatives. This corresponds to a non-local term resulting from the optimal choice for the constitutive equation. The terms deriving from I_x are easily evaluated if the form of the sought solution is chosen. Looking for $u(x)$ as exponentials :

$$u(x) = A_u e^{\alpha_u x} \quad (71)$$

yields

$$\begin{aligned} \bar{I}_x &= e^{\alpha_7 x} \int^x \frac{d^3 u}{dx^3}(\eta) e^{-\alpha_7 \eta} d\eta - e^{-\alpha_7 x} \int^x \frac{d^3 u}{dx^3}(\eta) e^{\alpha_7 \eta} d\eta \\ &= \frac{2A_u \alpha_u^3 \alpha_7}{\alpha_u^2 - \alpha_7^2} e^{\alpha_u x} + A_u \alpha_u^3 (K^+ e^{\alpha_7 x} - K^- e^{-\alpha_7 x}) \end{aligned} \quad (72)$$

where K^+ and K^- are to be determined. Similarly, setting

$$v(x) = A_v e^{\alpha_v x} \quad (73)$$

yields

$$\begin{aligned} \frac{-12}{t} \dot{I}_x &= e^{\alpha_7 x} \int^x \frac{d^4 v}{dx^4}(\eta) e^{-\alpha_7 \eta} d\eta - e^{-\alpha_7 x} \int^x \frac{d^4 v}{dx^4}(\eta) e^{\alpha_7 \eta} d\eta \\ &= \frac{2A_v \alpha_v^4 \alpha_7}{\alpha_v^2 - \alpha_7^2} e^{\alpha_v x} + A_v \alpha_v^4 (K'^+ e^{\alpha_7 x} - K'^- e^{-\alpha_7 x}) \end{aligned} \quad (74)$$

and the Eq.(68) can be treated as usual.

- Compared to the equation obtained by a purely kinematic approach [33], the equation is also modified by the new C_{xx}^0 term, which also results from the optimality conditions. It links the surface energy to the Cauchy stress tensor through the cohesion modulus, and as such, represents a chemo-mechanical coupling. It thus modifies boundary conditions for the tension problem under chemical loading.

5. Solutions for purely mechanical problems

Two mechanical problems of practical interest are now solved using Eq.(68) in order to exhibit the size-dependent elasticity rendered by the beam theory under scrutiny.

5.1. Tension stiffness

5.1.1. Governing equations

One first focuses on the tension problem, for which the general solution $u(x)$ has to satisfy

$$\begin{aligned}
C_{xxxx} \frac{d^6 u}{dx^6} + (C_{xxx}^{xxx} + C_{xxx}^{xx} - C_{xxx}^{xxx}) \frac{d^4 u}{dx^4} \\
+ C_{xx}^{xx} \frac{d^2 u}{dx^2} + C_{xx}^{ix} \frac{d \bar{I}_x}{dx} + C_{xxxx}^{ix} \frac{d^3 \bar{I}_x}{dx^3} = 0 \quad \forall x \in [0, L] \quad (75)
\end{aligned}$$

It should be outlined that this equation clearly departs from an analogue of the 3D constitutive laws [21], and this results from the static admissibility conditions. Looking for solutions of the form (71) yields the characteristic equation

$$\begin{aligned}
0 = & \left\{ \left(C_{xxxx}^{xxx} + \frac{2C_{xxxx}^{ix} \alpha_7}{\alpha_u^2 - \alpha_7^2} \right) \alpha_u^6 + \left(C_{xxx}^{xxx} + C_{xxx}^{xx} - C_{xxx}^{xxx} + \frac{2C_{xxx}^{ix} \alpha_7}{\alpha_u^2 - \alpha_7^2} \right) \alpha_u^4 + C_{xx}^{xx} \alpha_u^2 \right\} e^{\alpha_u x} \\
& + \alpha_u^3 \alpha_7 (C_{xx}^{ix} + \alpha_7^2 C_{xxxx}^{ix}) (\bar{K}^+ e^{\alpha_7 x} + \bar{K}^- e^{-\alpha_7 x}) \quad (76)
\end{aligned}$$

It is clear from Eq.(76) that $\alpha_u^2 = 0$ is a trivial solution, and that the equation obtained by multiplying Eq.(76) by $\frac{\alpha_u^2 - \alpha_7^2}{\alpha_u^2}$, has solutions if $\bar{K}^- = \bar{K}^+ = 0$. One thus obtains

$$\begin{aligned} C_{xxxx} \alpha_u^6 + (C_{xx}^{xxxx} + C_{xxxx}^{xx} - C_{xxx}^{xxx} + 2C_{xxxx}^{ix} \alpha_7 - \alpha_7^2 C_{xxxx}^{xxxx}) \alpha_u^4 + \\ (2C_{xx}^{ix} \alpha_7 - \alpha_7^2 (C_{xx}^{xxxx} + C_{xxxx}^{xx} - C_{xxx}^{xxx}) + C_{xx}^{xx}) \alpha_u^2 - \alpha_7^2 C_{xx}^{xx} = 0 \end{aligned} \quad (77)$$

The solutions therefore read

$$\alpha_u = \{ \pm \lambda_{u,1}^{-1}, \pm \lambda_{u,2}^{-1}, \pm \lambda_{u,3}^{-1}, 0 \} \quad (78)$$

where $\lambda_{u,1}$, $\lambda_{u,2}$ and $\lambda_{u,3}$ are generally complex numbers scaling as lengths. The general solution $u(x)$ therefore reads

$$u(x) = \sum_{i=0}^1 q_i x^i + \sum_{j=1}^3 \gamma_j^+ \exp\left(\frac{x}{\lambda_{u,j}}\right) + \gamma_j^- \exp\left(-\frac{x}{\lambda_{u,j}}\right) \quad (79)$$

$\{q_i, \gamma_j^+, \gamma_j^-\}$, are the 8 constants to be set from the boundary conditions. However, only 6 boundary conditions are obtained from Eq.(68). Assuming the beam is clamped at $x = 0$, these boundary conditions read

$$\begin{aligned} u(0) &= 0 \\ C_{xxxx} \frac{d^4 u}{dx^4}(0) + (C_{xx}^{xxxx} - C_{xxx}^{xxx}) \frac{d^2 u}{dx^2}(0) + C_{xxxx}^{ix} \frac{d \bar{I}_x}{dx}(0) &= 0 \\ C_{xxxx} \frac{d^3 u}{dx^3}(0) + C_{xxxx}^{xx} \frac{du}{dx}(0) + C_{xxxx}^{ix} \bar{I}_x(0) &= 0 \end{aligned}$$

Extending to second-strain gradient elasticity the terms coined in [42], this would correspond to a singly clamped beam at $x = 0$. A tensile force F is applied at $x = L$, the work of external forces reads $\delta W^* = F u^*(x = L)$ so

that

$$\begin{aligned}
C_{xxxx} \frac{d^5 u}{dx^5}(L) + (C_{xx}^{xxxx} + C_{xxxx}^{xx} - C_{xxx}^{xxx}) \frac{d^3 u}{dx^3}(L) \\
+ C_{xx}^{xx} \frac{du}{dx}(L) + C_{xx}^{ix} \bar{I}_x(L) + C_{xxxx}^{ix} \frac{d^2 \bar{I}_x}{dx^2}(L) &= \frac{F}{bt} \\
C_{xxxx} \frac{d^4 u}{dx^4}(L) + (C_{xxxx}^{xx} - C_{xxx}^{xxx}) \frac{d^2 u}{dx^2}(L) + C_{xxxx}^{ix} \frac{d \bar{I}_x}{dx}(L) &= 0 \\
C_{xxxx} \frac{d^3 u}{dx^3}(L) + C_{xxxx}^{xx} \frac{du}{dx}(L) + C_{xxxx}^{ix} \bar{I}_x(L) &= 0
\end{aligned}$$

These conditions would actually be denoted as triply free if one extends the nomenclature in [42]. These 6 conditions are obviously not sufficient to yield a unique solution. It is evident this results from the non-local terms in the optimal constitutive equations. Denoting

$$\begin{aligned}
S_j &= -\frac{\alpha_7^2 (C_{xxx}^{xxx} - C_{xxxx}^{xx}) \lambda_{u,j}^4 + (C_{xxxx}^{xx} - C_{xxx}^{xxx} - \alpha_7^2 C_{xxxx}^{xxxx} + 2\alpha_7 C_{xxxx}^{ix}) \lambda_{u,j}^2 + C_{xxxx}^{xxxx}}{\lambda_{u,j}^4 (\alpha_7 \lambda_{u,j} - 1) (\alpha_7 \lambda_{u,j} + 1)} \\
T_j &= \frac{\alpha_7^2 C_{xxxx}^{xx} \lambda_{u,j}^4 + (\alpha_7^2 C_{xxxx}^{xxxx} - C_{xxxx}^{xx} - 2\alpha_7 C_{xxxx}^{ix}) \lambda_{u,j}^2 - C_{xxxx}^{xxxx}}{\lambda_{u,j}^3 (\alpha_7 \lambda_{u,j} - 1) (\alpha_7 \lambda_{u,j} + 1)}
\end{aligned}$$

the linear system to be solved reads

$$\begin{bmatrix}
1 & 0 & 1 & 1 & 1 & 1 & 1 & 1 \\
0 & 0 & S_1 & S_1 & S_2 & S_2 & S_3 & S_3 \\
0 & C_{xxxx}^{xx} & T_1 & -T_1 & T_2 & -T_2 & T_3 & -T_3 \\
0 & C_{xx}^{xx} & 0 & 0 & 0 & 0 & 0 & 0 \\
0 & 0 & S_1 e^{\frac{L}{\lambda_{u,1}}} & S_1 e^{-\frac{L}{\lambda_{u,1}}} & S_2 e^{\frac{L}{\lambda_{u,2}}} & S_2 e^{-\frac{L}{\lambda_{u,2}}} & S_3 e^{\frac{L}{\lambda_{u,3}}} & S_3 e^{-\frac{L}{\lambda_{u,3}}} \\
0 & C_{xxxx}^{xx} & T_1 e^{\frac{L}{\lambda_{u,1}}} & -T_1 e^{-\frac{L}{\lambda_{u,1}}} & T_2 e^{\frac{L}{\lambda_{u,2}}} & -T_2 e^{-\frac{L}{\lambda_{u,2}}} & T_3 e^{\frac{L}{\lambda_{u,3}}} & -T_3 e^{-\frac{L}{\lambda_{u,3}}}
\end{bmatrix} \mathbf{U} = \begin{bmatrix} 0 \\ 0 \\ 0 \\ \frac{F}{bt} \\ 0 \\ 0 \end{bmatrix} \quad (80)$$

where

$$\mathbf{U}^t = [q_0, q_1, \gamma_1^+, \gamma_1^-, \gamma_2^+, \gamma_2^-, \gamma_3^+, \gamma_3^-]^t \quad (81)$$

The full solution space for \mathbf{U} reads

$$\mathbf{U} = \mathbf{U}_m + \mathcal{U}_E \mathbf{P}_E \quad (82)$$

where the columns of \mathcal{U}_E span the nullspace of the matrix in Eq.(80). This solution space corresponds to the displacement fields :

- Locally satisfying the static admissibility,
- Locally minimizing the constitutive equation gap,
- Globally satisfying the static admissibility.

As the constitutive equations obtained in Sect.(3.2) differ from the 3D laws, the remaining constitutive equation gap is nonzero (see Sect.(4.1)), so that the fields defined by Eq.(82) are obviously not equivalent regarding the constitutive equation gap at the global (structure) scale. Accounting for the non-local terms in the constitutive equations thus requires to define the solution $\hat{\mathbf{P}}_E$ for \mathbf{P}_E as the minimizer of the global constitutive equation gap

$$\hat{\mathbf{P}}_E = \text{Arg min}_{\mathbf{P}_E} \int \eta_\psi (\mathcal{C}_{opt}^{EB} \mathbf{E}_{KA}(\mathbf{U}) + \mathbf{B}_{opt}^{EB}, \mathbf{E}_{KA}(\mathbf{U})) dV \quad (83)$$

As a consequence of Eq.(82), \mathbf{E}_{KA} formally reads

$$\mathbf{E}_{KA}(x) = \mathbf{E}_m(x) + \mathcal{M}_E(x) \mathbf{P}_E \quad (84)$$

which is built explicitly and solved to yield the solution $\hat{\mathbf{P}}_E$ under the constrain of real-valued displacement fields. The components of the displacement field are thus obtained

$$\hat{\mathbf{U}} = \mathbf{U}_m + \mathcal{U}_E \hat{\mathbf{P}}_E \quad (85)$$

It is worth noting that the solution here depends on b_0 . This results from the fact that tension modifies the total amount of surface of the sample, b_0 being the equivalent of surface tension for solids [19]. The normalized tensile stiffness

$$\frac{S_{SSG}}{S_{Cauchy}} = \frac{F L}{b t u(L) C_{xx}^{xx}} \quad (86)$$

may thus be computed to illustrate the scaling effect. It should be first mentioned that the equations of first-strain gradient are easily obtained in the present case by canceling all the SSG-related terms in Eq. (75). One obtains (in the absence of distributed loading)

$$\frac{C_{xxx}^{xxx}}{C_{xx}^{xx}} \frac{d^4 u}{dx^4} - \frac{d^2 u}{dx^2} = 0 \quad \forall x \in [0, L] \quad (87)$$

which is formally similar to the equation obtained using a purely kinematic approach [42] with a simplified constitutive equation [43] :

$$g^2 \frac{d^4 u}{dx^4} - \frac{d^2 u}{dx^2} = 0 \quad \forall x \in [0, L] \quad (88)$$

The main outcome of the proposed approach is thus the definition

$$g^2 = \frac{C_{xxx}^{xxx}}{C_{xx}^{xx}} \quad (89)$$

thus relating the parameters of the 3D constitutive law to the parameters of the equations governing the beam behavior. Using this first-strain gradient theory with the chosen boundary conditions yields exactly the same solution as for Cauchy materials for the tension problem. The sole effect of second-strain gradient elasticity is thus probed by this tensile test if second-strain gradient elasticity is used.

5.1.2. Application to the simulated materials

The quantities involved in the tension problem are now analyzed for a large number of material parameters sets. 999 material parameters sets have been obtained by generating parameters sets with $l_S = 1 \times 10^{-3}$ and keeping those yielding a positive definite stiffness tensor. These parameters sets can be scaled to physical ones by setting physical l_S values [44, 45, 46].

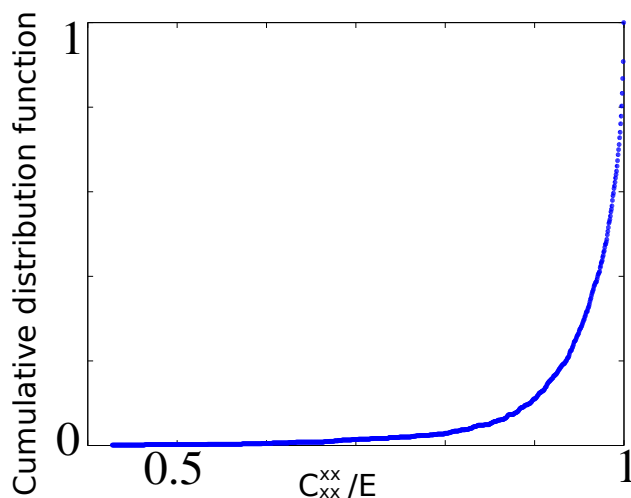


Figure 1: Cumulative distribution function for $\frac{C_{xx}^{xx}}{E}$.

The cumulative distribution function for $\frac{C_{xx}^{xx}}{E}$ is reported in Fig.1. The obtained values are always such that $C_{xx}^{xx} \leq E$. It should be noted that 73% of the tested materials yield $C_{xx}^{xx} \geq 0.95 \times E$. The cumulative distribution function for $|\alpha_7^2| \times l_S^2$ is reported in Fig 2. As already mentioned, α_7^2 is either positive or negative (yielding real or pure complex values for α_7), and α_7^2 may be considered to scale as l_S^{-2} since 61.5% of the tested materials yield $|\alpha_7^2| \times l_S^2 < 10$. The cumulative distribution function for $|\lambda_u|/l_S$ is shown in Fig. 3. It can be kept that $|\lambda_u|$ scales as l_S , since 98.5% of the tested

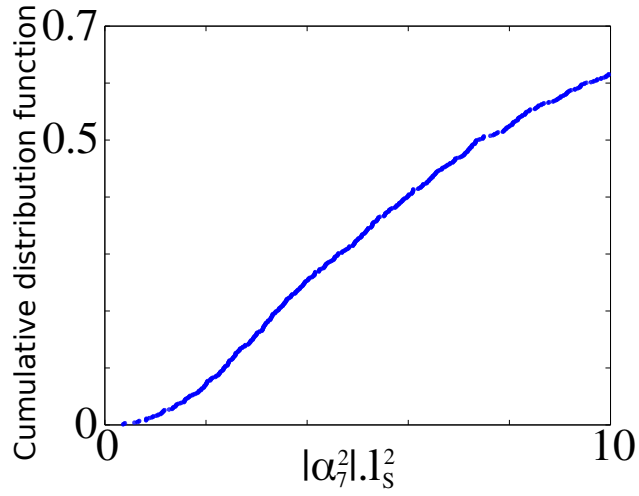


Figure 2: Cumulative distribution function for $|\alpha_7^2| \times l_S^2$.

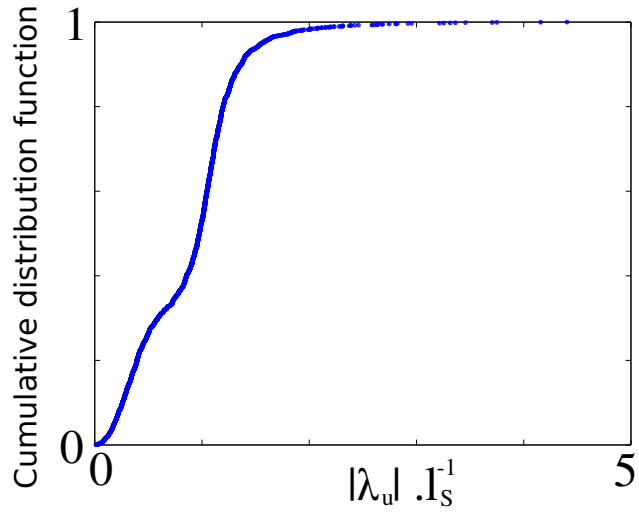


Figure 3: Cumulative distribution function for $|\lambda_u|/l_S$.

materials yield $|\lambda_u|/l_S < 2$. C_{xxx}^{xxx} is found to be always positive, and scales as $\mu \times l_S^2$, as seen in Fig. 4. C_{xxxx}^{xxx} and C_{xx}^{xxxx} are contrarily found to be either positive or negative. $|C_{xxxx}^{xx}|$ is found to scale as $\mu \times l_S^2$, as seen in Fig.

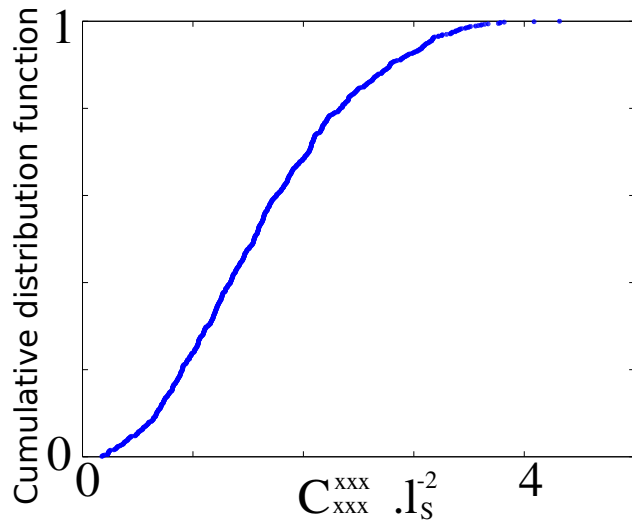


Figure 4: Cumulative distribution function for C_{xxx}^{xxx}/l_S^2 .

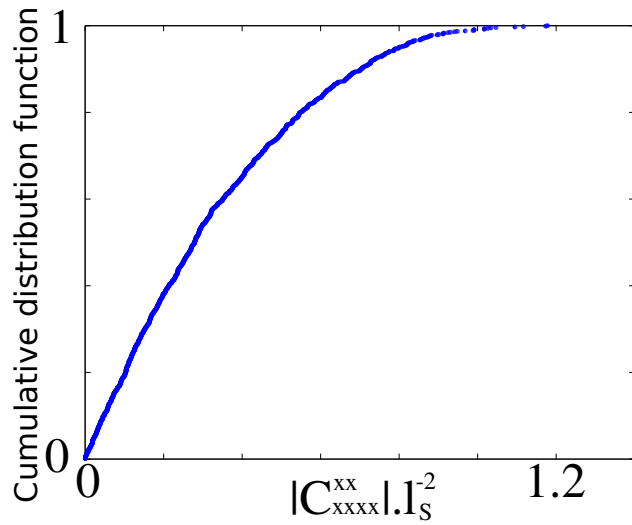


Figure 5: Cumulative distribution function for $|C_{xxx}^{xx}|/l_S^2$.

5. Similarly, $|C_{xx}^{xxxx}|$ is found to scale as $\mu \times l_S^2$, as seen in Fig. 6. C_{xxxx}^{xxxx} is also found to be either positive or negative, and scales as $\mu \times l_S^4$ (see Fig.

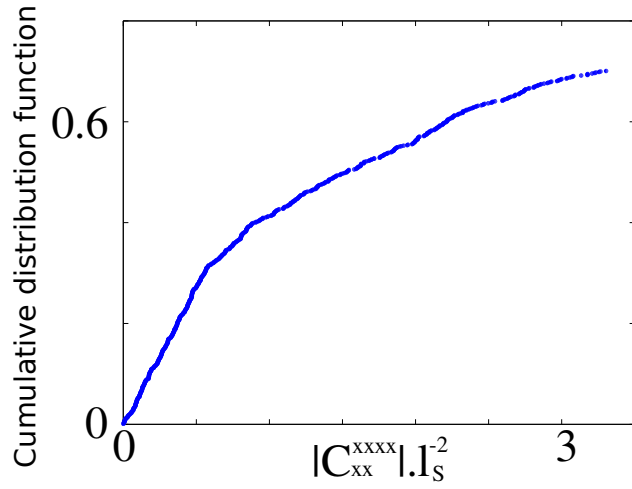


Figure 6: Cumulative distribution function for $|C_{xx}^{xxxx}|/l_S^2$.

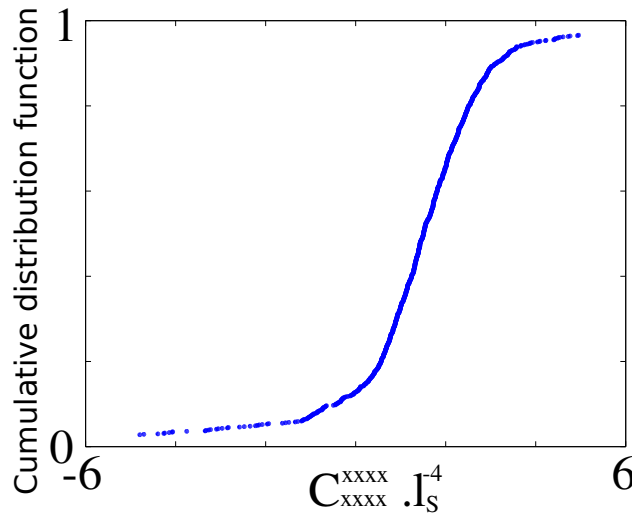


Figure 7: Cumulative distribution function for C_{xxxx}^{xxxx}/l_S^4 .

7). The products $\alpha_7 C_{xx}^{ix}$ and $\alpha_7 C_{xxxx}^{ix}$ are found to be always real. Even though its distribution is rather scattered, $\alpha_7 C_{xx}^{ix}$ is considered to scale as μ (see Fig. 8). Similarly, $\alpha_7 C_{xxxx}^{ix}$ is found to scale as $\mu \times l_S^2$ (see Fig. 9). Using

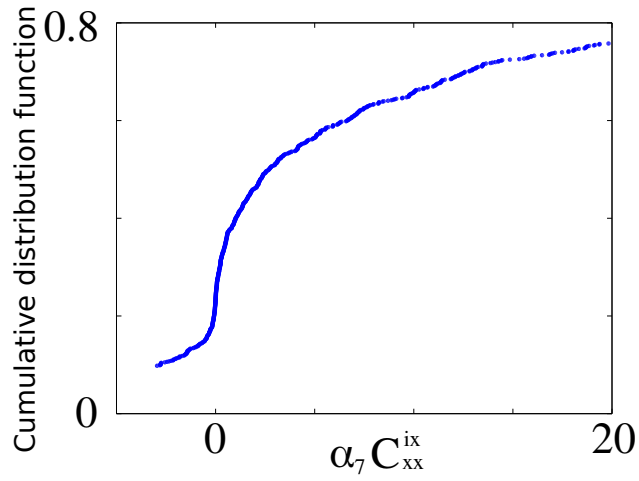


Figure 8: Cumulative distribution function for $\alpha_7 C_{xx}^{ix}$ (zoom).

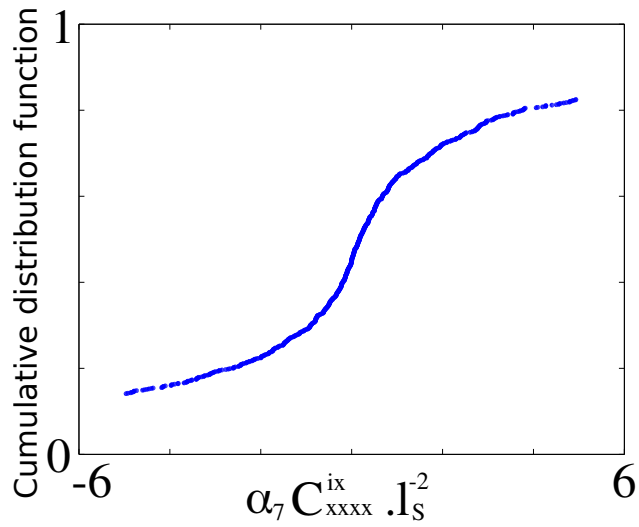


Figure 9: Cumulative distribution function for $\alpha_7 C_{xxxx}^{ix} / l_S^2$ (zoom).

all these coefficients, the tension stiffness of beams is computed following the procedure detailed in Sect. 5.1.1, as a function of the beam's length L and of the cohesion modulus b_0 .

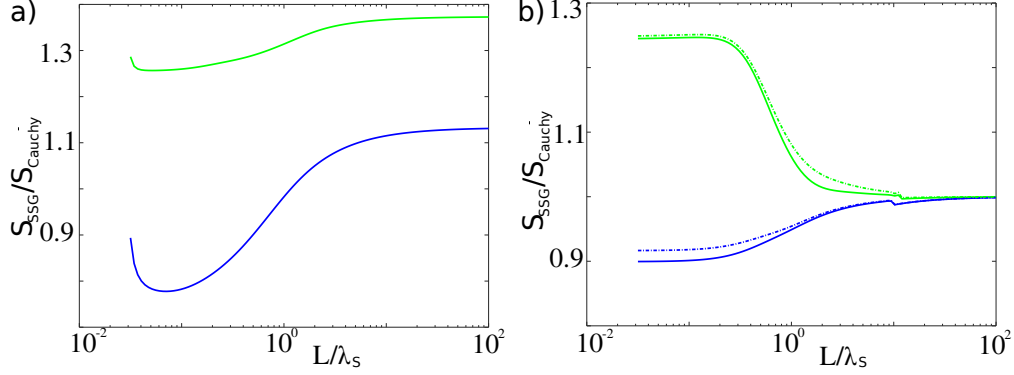


Figure 10: a) Normalized tension stiffnesses for 'blue' and 'green' materials (see Appendix E) using a purely kinematic approach. b) Normalized tension stiffnesses for 'blue' and 'green' materials and two different cohesion modulus values with the present approach : solid lines are for $b_0 = 0$, dashed lines are for $b_0 = l_S^2$.

Fig. 10a first shows two examples of the tension stiffness S_{SSG} obtained using a purely kinematic approach as described in [33], without any arbitrary rescaling. The used constitutive parameters are gathered in Appendix E. The beam's length is here normalized with respect to $\lambda_S = |\sum_j \lambda_{u,j}|$. It should be outlined that for $L \gg \lambda_S$, S_{SSG} does not converge to S_{Cauchy} . This is another illustration of the deficiency inherited of the purely kinematic construction already shown in [35]. The beam's tension stiffness actually tends to $(\lambda + 2\mu)S/L$ if the corresponding coefficient is not (arbitrarily) modified [33, 35]. The purpose of the present approach is to correct for such a deficiency and Fig. 10b displays two examples of the tension stiffness S_{SSG} obtained using the theory proposed herein, compared to the stiffness commonly obtained using Cauchy materials ($S_{Cauchy} = C_{xx}^{xx}S/L$). The solid lines are obtained by setting $b_0 = 0$, that is by discarding any surface tension. It

is first seen that for $L \gg \lambda_S$, $S_{SSG} \rightarrow S_{Cauchy}$ so that the usual behavior is recovered. Using the approach proposed herein, the limit is actually shown to read $C_{xx}^{xx}S/L$ (where the asymptotic behavior (67) holds). For $L \ll \lambda_S$, the tensile stiffness is driven by the higher-order elasticity parameters but the order in magnitude is preserved. The dashed lines are obtained by setting $b_0 = l_S^2$. This clearly affects the tensile stiffness in the $L \ll \lambda_S$ region, thereby highlighting the smaller beams are sensitive to surface elasticity in addition to bulk elasticity. λ_S may thus be used as the cross-over between two regimes for the elastic behavior of the beam : for beam lengths smaller than λ_S , the elasticity in tension is surface-driven, which it is proposed to denote as ecto-elastic (from ancient Greek “ektòs”, “outside”). If $L \gg \lambda_S$, the behavior is classically driven by the bulk.

Even though the cross-section dimensions do not appear explicitly in these results, it should be recalled that the proposed equations hold if the stresses fields belong to Θ (see Eq.(34)). The corresponding assumption could be assessed for specific dimensions using a dedicated numerical scheme, see [23] for instance.

5.2. Bending stiffness

5.2.1. Governing equations

One now focuses on the bending problem, for which the general solution $v(x)$ has to satisfy

$$C_{xxxx}^{xxxx} \frac{t^2}{12} \frac{d^8 v}{dx^8} + A \frac{d^6 v}{dx^6} + K \frac{d^4 v}{dx^4} - t \left(C_{xxxx}^{ix} \frac{d^4 \acute{I}_x}{dx^4} + C_{xx}^{ix} \frac{d^2 \acute{I}_x}{dx^2} \right) = 0 \quad \forall x \in [0, L] \quad (90)$$

with

$$A = \frac{t^2}{12} (C_{xx}^{xxxx} + C_{xxxx}^{xx} - C_{xxx}^{xxx}) - 2C_{xyx}^{xxxxy} + C_{xxy}^{xxxxy} + 3C_{xxyx}^{xxy} - C_{xxy}^{xxy} \quad (91)$$

$$K = C_{xxy}^{xxy} - 2C_{xyx}^{xxy} + \frac{C_{xx}^{xx}t^2}{12} \quad (92)$$

Looking for solutions of the form (73) yields the characteristic equation

$$0 = \alpha_v^4 \left\{ \left(C_{xxxx}^{xxxx} \frac{t^2}{12} \alpha_v^4 + A \alpha_v^2 + K + \frac{2\alpha_7 t^2}{12} \frac{\alpha_v^2 C_{xx}^{ix} + \alpha_v^4 C_{xxxx}^{ix}}{\alpha_v^2 - \alpha_7^2} \right) e^{\alpha_v x} + \frac{t^2 \alpha_7^2}{12} (C_{xx}^{ix} + \alpha_7^2 C_{xxxx}^{ix}) (K^+ e^{\alpha_7 x} - K^- e^{-\alpha_7 x}) \right\} \quad (93)$$

It is clear from Eq.(93) that $\alpha_v^4 = 0$ is a trivial solution, and that the equation obtained by multiplying Eq.(93) by $\frac{\alpha_v^2 - \alpha_7^2}{\alpha_v^4}$, has solutions if $K^- = K^+ = 0$. One thus obtains

$$C_{xxxx}^{xxxx} \frac{t^2}{12} \alpha_v^6 + \left(A - \alpha_7^2 C_{xxxx}^{xxxx} \frac{t^2}{12} + \frac{t^2}{6} \alpha_7 C_{xxxx}^{ix} \right) \alpha_v^4 + \left(K - A \alpha_7^2 + \frac{t^2}{6} \alpha_7 C_{xx}^{ix} \right) \alpha_v^2 - K \alpha_7^2 = 0 \quad (94)$$

The $t \rightarrow 0$ limit should be considered. For $t = 0$, the characteristic polynomial simplifies as

$$A_0 \alpha_v^4 + (K_0 - A_0 \alpha_7^2) \alpha_v^2 - K_0 \alpha_7^2 = 0 \quad (95)$$

with

$$A_0 = -2C_{xyx}^{xxxxy} + C_{xxy}^{xxxxy} + 3C_{xxyx}^{xxy} - C_{xxy}^{xxy} \quad (96)$$

$$K_0 = C_{xxy}^{xxy} - 2C_{xyx}^{xxy} \quad (97)$$

and thus defines two finite solutions

$$\alpha_v^2 = \frac{-K_0 + A_0 \alpha_7^2 \pm |K_0 + A_0 \alpha_7^2|}{2A_0} \quad (98)$$

It is easily checked that the third solution reads

$$\alpha_v^2 \simeq -\frac{12A_0}{C_{xxxx}}t^{-2} \quad (99)$$

for a vanishing thickness. In general, the solutions read

$$\alpha_v = \{\pm\lambda_{v,1}^{-1}, \pm\lambda_{v,2}^{-1}, \pm\lambda_{v,3}^{-1}, 0\} \quad (100)$$

where $\lambda_{v,1}$, $\lambda_{v,2}$ and $\lambda_{v,3}$ are generally complex numbers scaling as lengths.

The general solution $v(x)$ therefore reads

$$v(x) = q_0 + \sum_{i=1}^3 \frac{q_i}{i} \left(\frac{x}{L}\right)^i + \sum_{j=1}^3 \gamma_j^+ \exp\left(\frac{x}{\lambda_{v,j}}\right) + \gamma_j^- \exp\left(-\frac{x}{\lambda_{v,j}}\right) \quad (101)$$

$\{q_i, \gamma_j^+, \gamma_j^-\}$, are the 10 constants to be set from the boundary conditions.

However, only 8 boundary conditions are obtained from Eq.(68). Assuming

the beam is clamped at $x = 0$, these boundary conditions read

$$\begin{aligned} v(0) &= 0 \\ \frac{dv}{dx}(0) &= 0 \\ C_{xxxx} \frac{t^2}{12} \frac{d^5v}{dx^5}(0) + J \frac{d^3v}{dx^3}(0) - t C_{xxxx}^{ix} \frac{dI_x}{dx}(0) &= 0 \\ C_{xxxx} \frac{t}{12} \frac{d^4v}{dx^4}(0) + C_{xxxx}^{xx} \frac{t}{12} \frac{d^2v}{dx^2}(0) - C_{xxxx}^{ix} I_x(0) &= 0 \end{aligned}$$

with

$$J = \frac{t^2}{12} (C_{xxxx}^{xx} - C_{xxxx}^{xxx}) + 3C_{xxxx}^{xxy} - C_{xxxx}^{xxy} \quad (102)$$

Again extending to second-strain gradient elasticity the terms coined in [47]

for first strain-gradient elasticity, this would correspond to singly clamped

beam at $x = 0$. A bending force F is applied at $x = L$, the work of external

forces reads $\delta W^* = Fv^*(x = L)$ so that

$$\begin{aligned}
C_{xxxx} \frac{t^2}{12} \frac{d^7 v}{dx^7}(L) + A \frac{d^5 v}{dx^5}(L) + K \frac{d^3 v}{dx^3}(L) - t \left(C_{xxxx}^{ix} \frac{d^3 \acute{I}_x}{dx^3}(L) + C_{xx}^{ix} \frac{d \acute{I}_x}{dx}(L) \right) &= -\frac{F}{bt} \\
C_{xxxx} \frac{t^2}{12} \frac{d^6 v}{dx^6}(L) + \frac{d^4 v}{dx^4}(L) + K \frac{d^2 v}{dx^2}(L) - t \left(C_{xxxx}^{ix} \frac{d^2 \acute{I}_x}{dx^2}(L) + C_{xx}^{ix} \acute{I}_x(L) \right) &= 0 \\
C_{xxxx} \frac{t^2}{12} \frac{d^5 v}{dx^5}(L) + J \frac{d^3 v}{dx^3}(L) - t C_{xxxx}^{ix} \frac{d \acute{I}_x}{dx}(L) &= 0 \\
C_{xxxx} \frac{t}{12} \frac{d^4 v}{dx^4}(L) + C_{xxxx}^{ix} \frac{t}{12} \frac{d^2 v}{dx^2}(L) - C_{xxxx}^{ix} \acute{I}_x(L) &= 0
\end{aligned}$$

These boundary conditions would be denoted as free if one extends the proposition in [47]. These 8 conditions are obviously not sufficient to yield a unique solution. This again results from the non-local terms in the optimal constitutive equations. Denoting

$$\acute{S}_j = \frac{\alpha_7 C_{xxxx}^{ix} t}{6\lambda_{v,j}^2 (1 - \alpha_7^2 \lambda_{v,j}^2)} + \frac{C_{xxxx}^{ix} t}{12\lambda_{v,j}^2} + \frac{C_{xxxx}^{ix} t}{12\lambda_{v,j}^4} \quad (103)$$

$$\acute{T}_j = \frac{J}{\lambda_{v,j}^3} + \frac{\alpha_7 C_{xxxx}^{ix} t^2}{6\lambda_{v,j}^3 (1 - \alpha_7^2 \lambda_{v,j}^2)} + \frac{C_{xxxx}^{ix} t^2}{12\lambda_{v,j}^5} \quad (104)$$

$$\acute{U}_j = \frac{K}{\lambda_{v,j}^3} + \frac{A}{\lambda_{v,j}^5} + \frac{\alpha_7 t^2}{6\lambda_{v,j}^2 (1 - \alpha_7^2 \lambda_{v,j}^2)} \left(\frac{C_{xx}^{ix}}{\lambda_{v,j}} + \frac{C_{xxxx}^{ix}}{\lambda_{v,j}^3} \right) + \frac{C_{xxxx}^{ix} t^2}{12\lambda_{v,j}^7} \quad (105)$$

the linear system to be solved reads

$$\begin{bmatrix}
1 & 0 & 0 & 0 & 1 & 1 & 1 & 1 & 1 & 1 \\
0 & L^{-1} & 0 & 0 & \lambda_{v,1}^{-1} & -\lambda_{v,1}^{-1} & \lambda_{v,2}^{-1} & -\lambda_{v,2}^{-1} & \lambda_{v,3}^{-1} & -\lambda_{v,3}^{-1} \\
0 & 0 & 0 & 2JL^{-3} & \acute{T}_1 & -\acute{T}_1 & \acute{T}_2 & -\acute{T}_2 & \acute{T}_3 & -\acute{T}_3 \\
0 & 0 & \frac{C_{xxxx}^{ix} t}{12L^2} & 0 & \acute{S}_1 & \acute{S}_1 & \acute{S}_2 & \acute{S}_2 & \acute{S}_3 & \acute{S}_3 \\
0 & 0 & 0 & 2KL^{-3} & \acute{U}_1 e^{\frac{L}{\lambda_{v,1}}} & -\acute{U}_1 e^{-\frac{L}{\lambda_{v,1}}} & \acute{U}_2 e^{\frac{L}{\lambda_{v,2}}} & -\acute{U}_2 e^{-\frac{L}{\lambda_{v,2}}} & \acute{U}_3 e^{\frac{L}{\lambda_{v,3}}} & -\acute{U}_3 e^{-\frac{L}{\lambda_{v,3}}} \\
0 & 0 & KL^{-2} & 2KL^{-2} & \acute{U}_1 \lambda_{v,1} e^{\frac{L}{\lambda_{v,1}}} & \acute{U}_1 \lambda_{v,1} e^{-\frac{L}{\lambda_{v,1}}} & \acute{U}_2 \lambda_{v,2} e^{\frac{L}{\lambda_{v,2}}} & \acute{U}_2 \lambda_{v,2} e^{-\frac{L}{\lambda_{v,2}}} & \acute{U}_3 \lambda_{v,3} e^{\frac{L}{\lambda_{v,3}}} & \acute{U}_3 \lambda_{v,3} e^{-\frac{L}{\lambda_{v,3}}} \\
0 & 0 & 0 & 2JL^{-3} & \acute{T}_1 e^{\frac{L}{\lambda_{v,1}}} & -\acute{T}_1 e^{-\frac{L}{\lambda_{v,1}}} & \acute{T}_2 e^{\frac{L}{\lambda_{v,2}}} & -\acute{T}_2 e^{-\frac{L}{\lambda_{v,2}}} & \acute{T}_3 e^{\frac{L}{\lambda_{v,3}}} & -\acute{T}_3 e^{-\frac{L}{\lambda_{v,3}}} \\
0 & 0 & \frac{C_{xxxx}^{ix} t}{12L^2} & \frac{C_{xxxx}^{ix} t}{6L^2} & \acute{S}_1 e^{\frac{L}{\lambda_{v,1}}} & \acute{S}_1 e^{-\frac{L}{\lambda_{v,1}}} & \acute{S}_2 e^{\frac{L}{\lambda_{v,2}}} & \acute{S}_2 e^{-\frac{L}{\lambda_{v,2}}} & \acute{S}_3 e^{\frac{L}{\lambda_{v,3}}} & \acute{S}_3 e^{-\frac{L}{\lambda_{v,3}}}
\end{bmatrix} \mathbf{v} = \begin{bmatrix} 0 \\ 0 \\ 0 \\ 0 \\ -\frac{F}{bt} \\ 0 \\ 0 \\ 0 \\ 0 \\ 0 \end{bmatrix} \quad (106)$$

where

$$\mathbf{V}^t = [q_0, q_1, q_2, q_3 \gamma_1^+, \gamma_1^-, \gamma_2^+, \gamma_2^-, \gamma_3^+, \gamma_3^-]^t \quad (107)$$

The full solution space for \mathbf{V} reads

$$\mathbf{V} = \mathbf{V}_m + \mathcal{V}_E \mathbf{R}_E \quad (108)$$

where the columns of \mathcal{V}_E span the nullspace of the matrix above. A unique solution for \mathbf{V} is again obtained as the minimizer of the total constitutive equation gap in the beam (see Eq.(83)). The linear system provided by the stationarity condition is again built explicitly and solved to yield the solution $\hat{\mathbf{R}}_E$ under the constrain of real-valued displacement fields. The components of the displacement field are thus obtained

$$\hat{\mathbf{V}} = \mathbf{V}_m + \mathcal{V}_E \hat{\mathbf{R}}_E \quad (109)$$

The main difference is that for the bending of a beam with a symmetric cross-section, the b_0 related terms are found to vanish. This is the expected behavior : in such case, the total amount of beam's surface remains unchanged by the deformation, so that the solution is always insensitive to the surface elasticity. The normalized bending stiffness

$$\frac{K_V^{SSG}}{K_V^{Cauchy}} = \frac{4F L^3}{b t^3 v(L) C_{xx}^{xx}} \quad (110)$$

may thus be computed to illustrate the scaling effect, which can be compared to the one predicted by first-strain gradient elasticity (see Appendix D) or Cauchy elasticity.

5.2.2. Application to the simulated materials

Reusing the material parameters sets generated in Sect.(5.1.2), the quantities involved in the bending problem are analyzed. The scale effect is then assessed in two steps of increasing complexity : the results for the present

theory applied keeping only Cauchy and first-strain gradient terms are first analyzed, and then serve as a reference when analyzing the results obtained when including second-strain gradient elasticity.

First-strain gradient elasticity. The solution for the bending problem in first-strain gradient elasticity is derived in Appendix D. The key parameters are now reviewed. Fig. 11 displays the cumulative distribution function

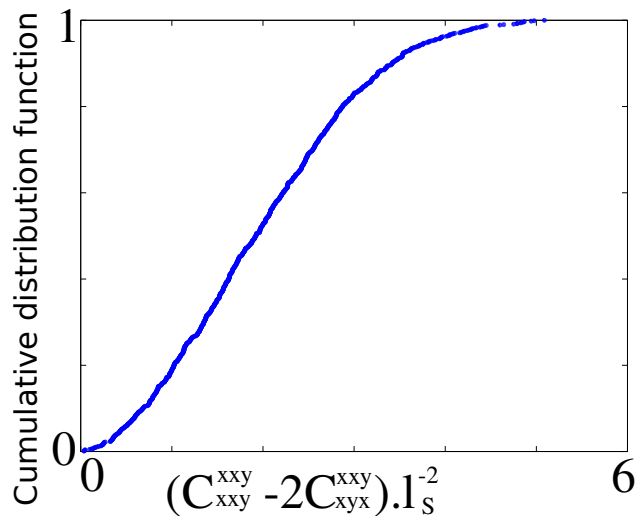


Figure 11: Cumulative distribution function for $(C_{xxy}^{xxy} - 2C_{xyx}^{xxy}) \times l_S^{-2}$.

for $(C_{xxy}^{xxy} - 2C_{xyx}^{xxy}) \times l_S^{-2}$. It may be seen in particular that this term is always positive. The consequence is that K is always positive, so that the characteristic length λ_V , which depends on the material and on the beam thickness (see Appendix D), is always a real positive number. It converges to a constant value

$$\lim_{t \rightarrow +\infty} \lambda_V = \sqrt{\frac{C_{xxx}^{xxx}}{C_{xx}^{xx}}} = \lambda_V^\infty \quad (111)$$

for large thicknesses and is proportional to the beam thickness in the vanishing thickness limit

$$\lambda_V \underset{t=0}{\propto} t \sqrt{\frac{C_{xxx}^{xxx}}{12(C_{xxy}^{xxy} - 2C_{xyx}^{xxy})}} = \hat{\lambda}_0 t \quad (112)$$

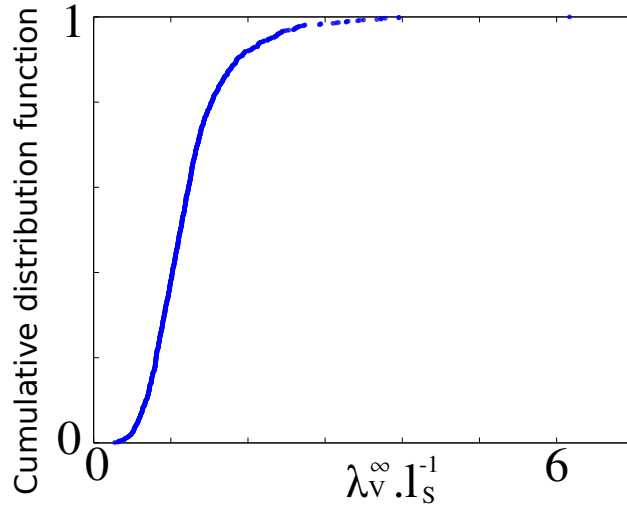


Figure 12: Cumulative distribution function for $\lambda_V^\infty \times l_S^{-1}$.

λ_V^∞ is shown to scale as l_S (see Fig. 12) and $\hat{\lambda}_0$ scales as unity (see Fig. 13). In the sequel, the investigated thickness range is defined with respect to

$$t_T = \sqrt{\frac{12(C_{xxy}^{xxy} - 2C_{xyx}^{xxy})}{C_{xx}^{xx}}} \quad (113)$$

so that $t \gg t_T$ implies that $K \propto \frac{C_{xx}^{xx} t^2}{12}$, whereas $t \ll t_T$ corresponds to $K \propto C_{xxy}^{xxy} - 2C_{xyx}^{xxy}$ (see Eq. 92).

Fig. 14 thus illustrates these two regimes on the λ_V value for two particular materials. Fig 15 illustrates the effect of both the cantilever's thickness

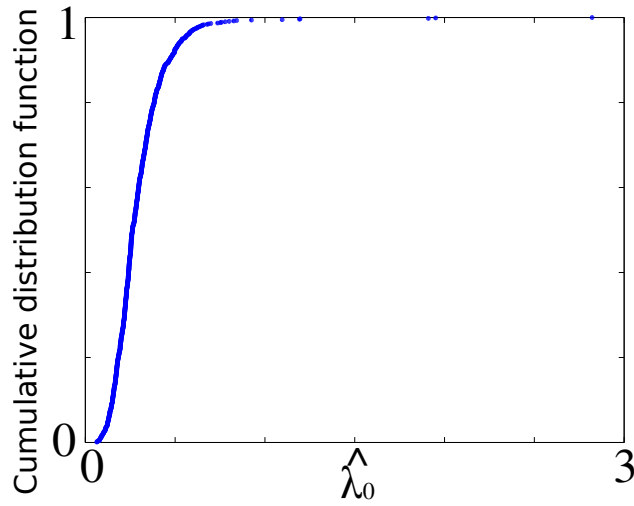


Figure 13: Cumulative distribution function for $\hat{\lambda}_0$.

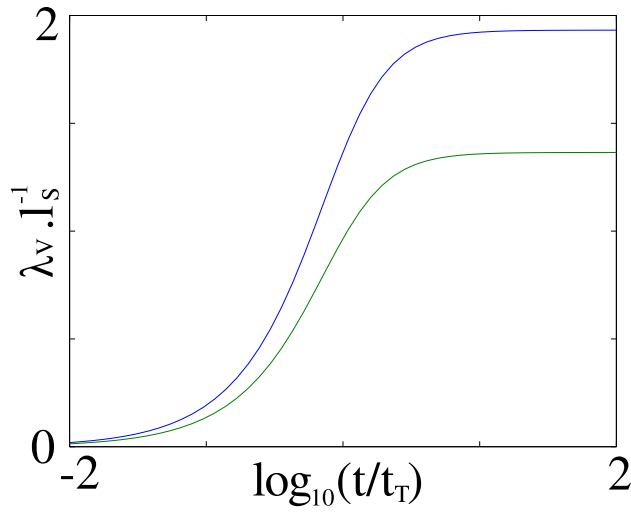


Figure 14: $\lambda_V \times l_S^{-1}$ as a function of $\log_{10}(t/t_T)$ for the materials of Fig. 10.

and length on the normalized bending stiffness for the “blue” material of Fig. 10. As the beam geometry imposes that $L \gg t$, the normalized bending stiff-

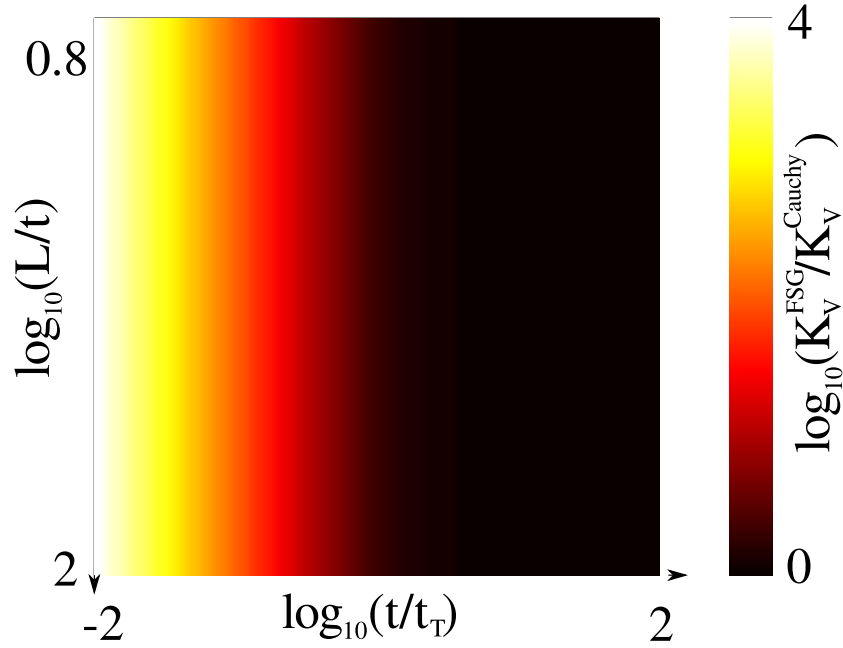


Figure 15: $\log_{10}(K_V^{FSG}/K_V^{Cauchy})$ as a function of $\log_{10}(t/t_T)$ and $\log_{10}(L/t)$ for “blue” material of Fig. 10.

ness is shown for lengths L such as $5t \leq L \leq 100t$. As a single characteristic length (λ_V) is involved, it is clear that the cantilever’s thickness is the main parameter driving the size-dependent elasticity. This is further illustrated on Fig. 16 on which $\log_{10}(K_V^{FSG}/K_V^{Cauchy})$ is plotted as a function of $\log_{10}(t/t_T)$ for $L = 10 \times t$ for blue material of Fig. 10. $t \gg t_T$ corresponds to a regime where the size-effect vanishes, whereas the domain $t \ll t_T$ is characterized by $\frac{K_V^{FSG}}{K_V^{Cauchy}} \propto \left(\frac{t}{t_T}\right)^{-2}$. Decreasing the cantilever’s thickness is always found to yield an apparent stiffening of the beam. The beam’s length has a negligible role : in the probed lengths range, its impact on the flexural beam stiffness is below 1%.

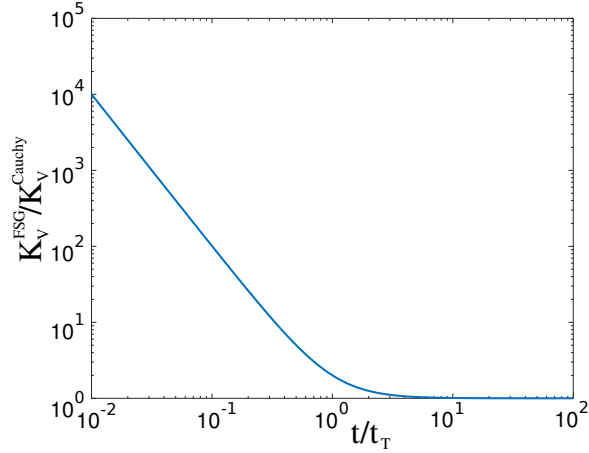


Figure 16: $\log_{10}(K_V^{FSG}/K_V^{Cauchy})$ as a function of $\log_{10}(t/t_T)$ for $L = 10 \times t$ for “blue” material of Fig. 10.

The results for the first-strain gradient elasticity are rather simple and thus provide a first step to further elaborate on results obtained with higher-order elasticity. As for bars, the proposed approach extends the validity range of the differential equations obtained with a simplified constitutive equation (see Appendix D).

Second-strain gradient elasticity. It is chosen for the sake of robustness to obtain \mathbf{V}_m by removing the two columns of the matrix in Eq.(106) corresponding to the $\lambda_{v,i}$ with the smallest norm, thus avoiding to make use of the $\lambda_{v,i}$ vanishing when t goes to 0. It should actually be noted that for t much larger than t_T , about 57% of the materials are found to result in at least one pure imaginary $\lambda_{v,i}$. This means that the displacement field may possibly be ‘decorated’ with a sinusoidal term all along the beam, provided that the beam length and the loading allow this deformation mode to develop.

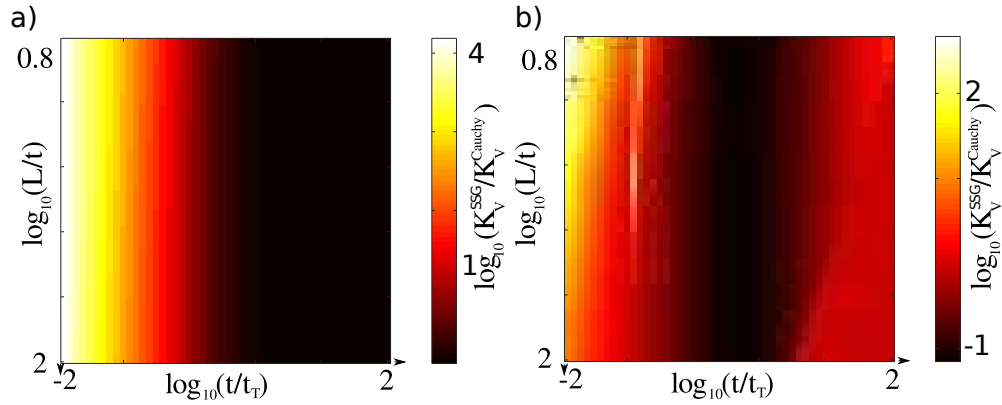


Figure 17: a) $\log_{10}(K_V^{SSG}/K_V^{Cauchy})$ as a function of $\log_{10}(t/t_T)$ and $\log_{10}(L/t)$ for blue material of Fig. 10 using a purely kinematic approach. b) $\log_{10}(K_V^{SSG}/K_V^{Cauchy})$ as a function of $\log_{10}(t/t_T)$ and $\log_{10}(L/t)$ for the same material using the present approach.

Fig. 17a displays the normalized bending stiffness $\log_{10}(K_V^{SSG}/K_V^{Cauchy})$ obtained using second-strain gradient elasticity for the material of Fig. 15 and a purely kinematic approach [33]. The computed stiffness is barely distinguishable from the one in Fig. 15, thereby suggesting a limited impact of second-strain gradient elasticity on the stiffness. In the large thickness regime ($t \gg t_T$), this stiffness however does not converge to 1, as a result of the deficiency already analyzed in Sect. 5.1.2. As it may be seen on Fig. 17b, the normalized bending stiffness $\log_{10}(K_V^{SSG}/K_V^{Cauchy})$ obtained using the present approach is mainly governed by the thickness value and converges to 1 for large thicknesses. This proves again that the built higher-grade beam theory is consistent with the usual beam theories, without any rescaling of the stiffness parameters to render the Poisson effect. It can also be seen that both the cantilever's length and thickness play a role in the beam bending stiffness, even though the thickness is the main driving parameter.

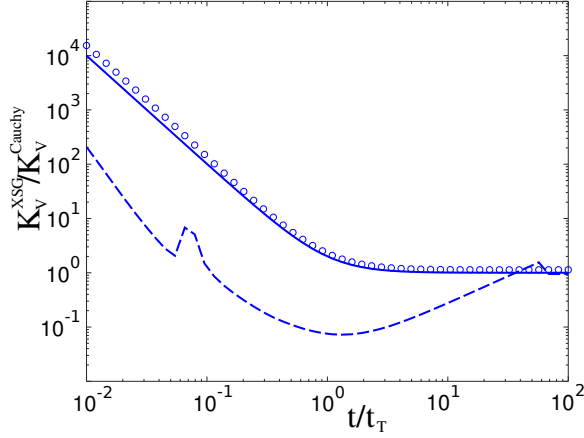


Figure 18: $\log_{10}(K_V^{SSG}/K_V^{Cauchy})$ (computed using a purely kinematic approach : dots, computed using the present approach : dashed line) and $\log_{10}(K_V^{FSG}/K_V^{Cauchy})$ (solid line) as a function of $\log_{10}(t/t_T)$ for $L = 10 \times t$ for “blue” material of Fig. 10.

The dependence of the normalized bending stiffness to the thickness is now non monotonic, as it may be seen on Fig. 17 and more precisely on Fig. 18, where both the normalized stiffnesses obtained for first and second strain-gradient elasticity (computed using a purely kinematic and the present approach) have been reported for the same material and the same dimensional range. The key result is that both grades affect the bending stiffness in the same dimensional range. This is clearly missed if one uses a purely kinematic approach, as the stiffness is then always very close to the one obtained using the first-strain gradient elasticity. This is however of major importance, since most of the reported experimental results regarding size-dependent elasticity deal with cantilever bending. The consequence is that both should always be considered simultaneously when analyzing experimental results, and that second-strain gradient elasticity should not be

considered, in general, as a correction to first-strain gradient elasticity which would be significant only for the smallest dimensions. This results from the fact that second-strain gradient introduces a coupling (through the c_i parameters) between second strain-gradient and Cauchy elasticity, which is absent from first-strain gradient elasticity.

6. Conclusion

Starting from the constitutive equation, beam equations have been derived for higher-grade elastic materials. The originality of this contribution stems from the fact that the static admissibility conditions are taken into account, so that these equations naturally converge to those classically obtained from Cauchy elasticity when the beam dimensions are large enough. The obtained equations thus benefit from the thermodynamic grounds of 3D elasticity and overcome the deficiencies resulting from a purely kinematic construction of the beam equations. The resulting material parameters are expressed as closed-forms, so that the resulting beam equations are kept very simple.

This approach has been exemplified on second-strain gradient elasticity with an Euler-Bernoulli kinematics, which is shown to result in non-local beam equations, whose shape function and characteristic length result from the 3D elastic parameters and are expressed as closed-forms. Second-strain gradient elasticity is of particular interest since it makes a cohesion modulus (*i.e.*, the equivalent of surface tension for solids) naturally appear. Such a framework is thus perfectly suited to describe scale effects one could wish to exploit for the design of innovative MEMS devices, and the rather simple approach pro-

posed herein allows for extensions to more complicated beam kinematics. In addition, applying the present approach to first-strain gradient elasticity formally confirms the differential equations obtained using a purely kinematic approach and a simplified constitutive equation. This extends their validity range and further provides the definition of the involved parameters.

Having a robust set of equations at hand to describe the behavior of higher-grade elastic beams allows to assess the role of the different grades on the size-dependent elasticity. As the tension problem only activates second-strain gradient elasticity, it is proposed to use it to define two elastic regimes. Namely, it allows to distinguish a regime (which it is proposed to denote as 'ecto-elastic') for which the tensile stiffness is driven by the cohesion modulus instead of being dominated by bulk elasticity. The beam length separating these two regimes has been defined as a function of the elastic parameters of the material under consideration. These governing equations for beams made of second strain-gradient elastic beams also suggest that second-strain gradient elasticity and first-strain gradient elasticity potentially affect the bending stiffness in the same dimensional range, so that both should always be considered simultaneously when analyzing experimental results.

This work is also expected to trigger some key developments for those interested in exploiting scale effects in solids :

- As outlined in Sect.4.4, and besides the effect on stiffness illustrated in Sect.5.1, the equations derived herein render the effect of a cohesion modulus change as an external loading. Equations obtained by following the proposed approach are thus expected to provide a framework which is adequate to model the chemo-mechanical couplings exploited

in micro-mechanical sensors. Even though this is out of the scope of this contribution, it is clear that this framework provides some crucial advantages for the understanding of the conversion phenomena at stake in cantilever-based sensors. Contrary to the widely used Stoney's equation, the role of the cantilever material in the chemo-mechanical transduction is here clearly described, and may explain the discrepancies observed in the literature [6].

- As it has been exemplified in Sect. 5, the solutions obtained using second-strain gradient elasticity involve responses at different scales, corresponding to the different grades. These are thus a starting point to devise experimental procedures aimed at identifying the higher-grade elastic parameters of materials. As such, this me paves the way to the experimental identification of the higher-order elastic parameters involved in the equations derived herein and defines a new challenge for experimental mechanics.

Appendix A. Euler-Bernoulli beam using 3D second-strain gradient elasticity

As recalled in the introduction, most of the beam equations derived in the literature for higher-grade elasticity are obtained by applying the 3D constitutive law to the (higher-order) strains derived from the chosen beam kinematics. The stresses obtained in this way are recalled hereafter for the sake of comparison with the optimal stresses derived in this contribution.

Solely using \mathcal{C}

$$\tau_{xx} = (\lambda + 2\mu) \epsilon_{xx} + (c_1 + c_2 + c_3) \epsilon_{xxxx} \quad (\text{A.1})$$

$$\tau_{xxx} = 2(a_1 + a_2 + a_3 + a_4 + a_5) \epsilon_{xxx} \quad (\text{A.2})$$

$$\tau_{xyx} = (a_1 + 2a_4 + a_5) \epsilon_{xyx} + \left(\frac{a_2}{2} + a_5\right) \epsilon_{xxy} \quad (\text{A.3})$$

$$\tau_{xxy} = (a_2 + 2a_5) \epsilon_{xyx} + 2(a_3 + a_4) \epsilon_{xxy} \quad (\text{A.4})$$

$$\begin{aligned} \tau_{xxxx} &= 2(b_1 + b_2 + b_3 + b_4 + b_5 + b_6 + b_7) \epsilon_{xxxx} \\ &\quad + \frac{b_3}{2} (\epsilon_{xxyx} + \epsilon_{xxxy}) + (c_1 + c_2 + c_3) \epsilon_{xx} + b_0 \end{aligned} \quad (\text{A.5})$$

$$\begin{aligned} \tau_{xxyx} &= \frac{2}{3} (2b_2 + b_3 + b_5 + 3b_6 + 2b_7) \epsilon_{xxyx} \\ &\quad + \frac{1}{3} (b_3 + 2b_4 + 2b_7) \epsilon_{xxxy} \end{aligned} \quad (\text{A.6})$$

$$\tau_{xxxy} = (b_3 + 2b_4 + 2b_7) \epsilon_{xxyx} + 2(b_5 + b_6) \epsilon_{xxxy} \quad (\text{A.7})$$

, so that without any consideration for static admissibility, the τ^1 components in the beam therefore read :

$$\tau_{xx}^{3D} = (\lambda + 2\mu) \left(-y \frac{d^2 v}{dx^2} + \frac{du}{dx} \right) + (c_1 + c_2 + c_3) \left(-y \frac{d^4 v}{dx^4} + \frac{d^3 u}{dx^3} \right) \quad (\text{A.8})$$

$$\tau_{xy}^{3D} = -c_2 \frac{d^3 v}{dx^3} \quad (\text{A.9})$$

$$\tau_{yy}^{3D} = \lambda \left(-y \frac{d^2 v}{dx^2} + \frac{du}{dx} \right) + (c_1 + c_2) \left(-y \frac{d^4 v}{dx^4} + \frac{d^3 u}{dx^3} \right) \quad (\text{A.10})$$

τ^2 :

$$\tau_{xxx}^{3D} = 2(a_1 + a_2 + a_3 + a_4 + a_5) \left(-y \frac{d^3 v}{dx^3} + \frac{d^2 u}{dx^2} \right) \quad (\text{A.11})$$

$$\tau_{yxx}^{3D} = \left(a_1 - \frac{a_2}{2} + 2a_4 \right) \left(-\frac{d^2 v}{dx^2} \right) \quad (\text{A.12})$$

$$\tau_{yyx}^{3D} = 2a_3 \left(-y \frac{d^3 v}{dx^3} + \frac{d^2 u}{dx^2} \right) \quad (\text{A.13})$$

$$\tau_{xxy}^{3D} = (-a_2 + 2a_3 + 2a_4 - 2a_5) \frac{d^2 v}{dx^2} \quad (\text{A.14})$$

$$\tau_{yxy}^{3D} = \left(a_1 + \frac{a_2}{2} \right) \left(-y \frac{d^3 v}{dx^3} + \frac{d^2 u}{dx^2} \right) \quad (\text{A.15})$$

$$\tau_{yyy}^{3D} = 2(-a_1 + a_3) \frac{d^2 v}{dx^2} \quad (\text{A.16})$$

τ^3 :

$$\begin{aligned}\tau_{xxxx}^{3D} &= 2(b_1 + b_2 + b_3 + b_4 + b_5 + b_6 + b_7) \left(-y \frac{d^4 v}{dx^4} + \frac{d^3 u}{dx^3} \right) \\ &\quad + (c_1 + c_2 + c_3) \left(-y \frac{d^2 v}{dx^2} + \frac{du}{dx} \right) + b_0\end{aligned}\quad (\text{A.17})$$

$$\tau_{yxxx}^{3D} = \frac{1}{3} (-4b_2 - b_3 + 2b_4 - 2b_5 - 6b_6 - 2b_7) \frac{d^3 v}{dx^3} \quad (\text{A.18})$$

$$\begin{aligned}\tau_{yyxx}^{3D} &= \frac{1}{3} (2b_1 + b_3 + 2b_4 + 2b_5) \left(-y \frac{d^4 v}{dx^4} + \frac{d^3 u}{dx^3} \right) \\ &\quad + \frac{1}{3} (c_1 + c_3) \left(-y \frac{d^2 v}{dx^2} + \frac{du}{dx} \right) + \frac{b_0}{3}\end{aligned}\quad (\text{A.19})$$

$$\tau_{yyyy}^{3D} = (-b_3 + 2b_4 - 2b_5) \frac{d^3 v}{dx^3} \quad (\text{A.20})$$

$$\tau_{xxxxy}^{3D} = (-b_3 - 2b_4 + 2b_5 + 2b_6 - 2b_7) \frac{d^3 v}{dx^3} \quad (\text{A.21})$$

$$\begin{aligned}\tau_{yxyx}^{3D} &= \frac{1}{3} (2b_1 + 2b_2 + b_3) \left(-y \frac{d^4 v}{dx^4} + \frac{d^3 u}{dx^3} \right) \\ &\quad + \frac{1}{3} (c_1 + c_2) \left(-y \frac{d^2 v}{dx^2} + \frac{du}{dx} \right) + \frac{b_0}{3}\end{aligned}\quad (\text{A.22})$$

$$\tau_{yyxy}^{3D} = \frac{1}{3} (-4b_2 - b_3 - 2b_4 + 2b_5) \frac{d^3 v}{dx^3} \quad (\text{A.23})$$

$$\tau_{yyyy}^{3D} = 2b_1 \left(-y \frac{d^4 v}{dx^4} + \frac{d^3 u}{dx^3} \right) + c_1 \left(-y \frac{d^2 v}{dx^2} + \frac{du}{dx} \right) + b_0 \quad (\text{A.24})$$

It should however be noted that Eq. (46) results from the stationarity conditions with respect to all the components of \mathbf{T}_Θ , including the last 12 ones which are derivatives of the others and are thus not independent (see definition (45)). One actually has to solve

$$\bar{\mathcal{P}}_\Theta^t \left(\mathcal{C}^{-1} \mathcal{P}_\Theta \hat{\mathbf{T}}_\Theta - \mathbf{E}_{KA} - \mathcal{C}^{-1} \mathbf{B} \right) = \mathbf{0} \quad (\text{B.3})$$

$\bar{\mathcal{P}}_\Theta$ is the restriction of \mathcal{P}_Θ to its 37 first columns. Similarly to \mathcal{P}_Θ , the SVD of $\bar{\mathcal{P}}_\Theta$ is easily obtained

$$\bar{\mathcal{P}}_\Theta = \bar{\mathcal{U}}_\Theta \bar{\mathcal{E}}_\Theta \bar{\mathcal{V}}_\Theta^t \quad (\text{B.4})$$

There are $54 - 37 = 17$ columns of $\bar{\mathcal{U}}_\Theta$ corresponding to null singular values of $\bar{\mathcal{P}}_\Theta$. These columns are thus concatenated in the 54×17 matrix $\bar{\mathcal{U}}_\perp$ which satisfies

$$\bar{\mathcal{U}}_\perp^t \bar{\mathcal{P}}_\Theta = \mathbf{0} \quad (\text{B.5})$$

Eq. (B.3) is then rewritten

$$\begin{aligned} \mathcal{C}^{-1} \mathcal{P}_\Theta \hat{\mathbf{T}}_\Theta - \mathbf{E}_{KA} - \mathcal{C}^{-1} \mathbf{B} &= \bar{\mathcal{U}}_\perp \bar{\mathbf{E}}_\perp \\ \mathcal{C} (\mathbf{E}_{KA} + \bar{\mathcal{U}}_\perp \bar{\mathbf{E}}_\perp) + \mathbf{B} &= \mathcal{P}_\Theta \hat{\mathbf{T}}_\Theta \end{aligned} \quad (\text{B.6})$$

where the vector $\bar{\mathbf{E}}_\perp$ is to be determined together with $\hat{\mathbf{T}}_\Theta$. Multiplying Eq. (B.6) by \mathcal{U}_\perp^t yields

$$\mathcal{U}_\perp^t (\mathcal{C} (\mathbf{E}_{KA} + \bar{\mathcal{U}}_\perp \bar{\mathbf{E}}_\perp) + \mathbf{B}) = \mathcal{U}_\perp^t \mathcal{P}_\Theta \hat{\mathbf{T}}_\Theta = \mathbf{0} \quad (\text{B.7})$$

This linear system is under-determined ($\mathcal{U}_\perp^t \mathcal{C} \bar{\mathcal{U}}_\perp$ is a 8×17 matrix), so that the solution reads

$$\bar{\mathbf{E}}_\perp = \bar{\mathbf{E}}_{\perp,0} + \bar{\mathcal{N}}_E \mathbf{Q} \quad (\text{B.8})$$

$\bar{\mathbf{E}}_{\perp,0}$ is obtained by inverting a 8×8 linear system, which is thus much smaller than the initial one (49×49) and does not require the inversion of \mathcal{C} . $\bar{\mathbf{E}}_{\perp,0}$ formally reads

$$\bar{\mathbf{E}}_{\perp,0} = \bar{\mathcal{E}}_{\perp,0}^B \mathbf{B} + \bar{\mathcal{E}}_{\perp,0}^E \mathbf{E}_{KA} \quad (\text{B.9})$$

$\bar{\mathcal{N}}_E$ is a 17×9 matrix which is easily built from the operator $\mathcal{U}_{\perp}^t \mathcal{C} \bar{\mathcal{U}}_{\perp}$, so that $\bar{\mathbf{E}}_{\perp}$ is easily obtained as a function of the 9 components of the vector \mathbf{Q} . The latter are to be determined. Defining $\check{\mathcal{E}}_{\Theta}^{-1}$ as the inverse of \mathcal{E}_{Θ} providing minimal norm solutions [48], Eq. (B.6) also yields the full solution space as

$$\hat{\mathbf{T}}_{\Theta} = \mathcal{N} \mathbf{t} + \mathcal{V}_{\Theta} \check{\mathcal{E}}_{\Theta}^{-1} \mathcal{U}_{\Theta}^t (\mathcal{C} (\mathbf{E}_{KA} + \bar{\mathcal{U}}_{\perp} (\bar{\mathbf{E}}_{\perp,0} + \bar{\mathcal{N}}_E \mathbf{Q})) + \mathbf{B}) \quad (\text{B.10})$$

The solution $\hat{\mathbf{T}}_{\Theta}$ is thus easily obtained and the constraints to be satisfied between the components of the result vector may be examined. Satisfying the 12 differential constraints between the components of $\hat{\mathbf{T}}_{\Theta}$ (see definition (45)) is presumably possible by setting the three components of \mathbf{t} and the nine components of \mathbf{Q} . One assumes hereafter that the material parameters are uniform. The solution obtained for the optimal constitutive equation after solving the differential equations resulting from Eq.(B.10) are given hereafter.

$$\begin{aligned} \tau_{xx} = & C_{xx}^{xx} \epsilon_{xx} + C_{xx}^{xxxx} \epsilon_{xxxx} + C_{xx}^0 b_0 \\ & + C_{xx}^{ix} \left(e^{\alpha_7 x} \int^x \epsilon_{xxxx}(\eta) e^{-\alpha_7 \eta} d\eta - e^{-\alpha_7 x} \int^x \epsilon_{xxxx}(\eta) e^{\alpha_7 \eta} d\eta \right) \end{aligned} \quad (\text{B.11})$$

where

$$C_{xx}^{xx} = \frac{\mu(3\lambda + 2\mu)(3b_7 + 3b_6 + 4b_5 + 4b_4 + 4b_3 + 4b_2 + 8b_1) - \lambda(c_2 + c_3)^2}{(\lambda + \mu)(3b_7 + 3b_6 + 4b_5 + 4b_4 + 4b_3 + 4b_2 + 8b_1) - (c_3 + c_2 + 2c_1)^2} + \frac{-2\mu((c_3 + c_2 + 2c_1)^2 + 2c_1^2)}{(\lambda + \mu)(3b_7 + 3b_6 + 4b_5 + 4b_4 + 4b_3 + 4b_2 + 8b_1) - (c_3 + c_2 + 2c_1)^2} \quad (\text{B.12})$$

$$Q_{xx}C_{xx}^{xxxx} = -\lambda(6(b_3 + 2b_2 + 2b_1)(b_7 + b_6) + 8(b_3 + 2b_2)(b_5 + b_4 + b_3 + b_2 + 3b_1)) + (4c_2(b_4 + b_5) - 3(b_7 + b_6)(c_3 + 2c_1))(c_1 + c_2 + c_3) + 2(b_3 + 2b_2)(c_3^2 + 5c_1c_3 + 6c_1^2) + 4(b_2 - 2b_1)c_2c_3 - 2(b_3 + 4b_1)c_2^2 + 2(3b_3 + 8b_2)c_1c_2 \quad (\text{B.13})$$

$$C_{xx}^0 = \frac{2(\lambda(c_3 + c_2) - 2c_1\mu)}{(\lambda + \mu)(3b_7 + 3b_6 + 4b_5 + 4b_4 + 4b_3 + 4b_2 + 8b_1) - (c_3 + c_2 + 2c_1)^2} \quad (\text{B.14})$$

$$C_{xx}^{ix} = \frac{6G_\epsilon(\lambda(3b_7 + 3b_6 + 4b_5 + 4b_4 + 4b_3 + 4b_2 + 8b_1) - 2c_1(c_3 + c_2 + 2c_1))}{2\alpha_7 Q_{xx}} \quad (\text{B.15})$$

$$G_\epsilon = \frac{2}{3} \left(\frac{2a_1 + a_2}{2} + \frac{2}{13} \frac{4b_1c_3 + 4b_1c_2 - (3b_7 + 3b_6 + 4b_5 + 4b_4 + 4b_3 + 4b_2)c_1}{3b_7 + 3b_6 + 4b_5 + 4b_4 + 4b_3 + 4b_2 + 8b_1} \right) - \alpha_7^2 \frac{3b_3b_7 + 6b_2b_7 + 6b_1b_7 + 3b_3b_6 + 6b_2b_6 + 6b_1b_6 + 4b_3b_5 + 8b_2b_5 + 4b_3b_4}{3(3b_7 + 3b_6 + 4b_5 + 4b_4 + 4b_3 + 4b_2 + 8b_1)} - \alpha_7^2 \frac{8b_2b_4 + 4b_3^2 + 12b_2b_3 + 12b_1b_3 + 8b_2^2 + 24b_1b_2}{3(3b_7 + 3b_6 + 4b_5 + 4b_4 + 4b_3 + 4b_2 + 8b_1)} - \alpha_7^{-2} \left(\frac{3}{13} \frac{((3b_7 + 3b_6 + 4b_5 + 4b_4 + 4b_3 + 4b_2 + 8b_1)\lambda - 2c_1c_3 - 2c_1c_2 - 4c_1^2)}{(3b_7 + 3b_6 + 4b_5 + 4b_4 + 4b_3 + 4b_2 + 8b_1)} + \frac{4}{39} \frac{(3b_7 + 3b_6 + 4b_5 + 4b_4 + 4b_3 + 4b_2 + 8b_1)\lambda - 2c_1c_3 - 2c_1c_2 - 4c_1^2}{3b_7 + 3b_6 + 4b_5 + 4b_4 + 4b_3 + 4b_2 + 8b_1} \right) \quad (\text{B.16})$$

$$Q_{xx} = (c_3 + 2c_1)(3b_7 + 3b_6 + 2b_3 + 4b_2) - c_2(4b_5 + 4b_4 + 2b_3 + 8b_1) \quad (\text{B.17})$$

$$\tau_{xz} = 0 = \tau_{yz} = \tau_{zy} \quad (\text{B.18})$$

$$\tau_{xy} = C_{xy}^{xxxy} \epsilon_{xxxy} = -C_2 \epsilon_{xxxy} \quad (\text{B.19})$$

$$\begin{aligned} \tau_{yy} &= (2C_{xyy}^{xxx} - 3C_{xyyy}^{xx} - 6\alpha_7 C_{xyyy}^{ix}) \epsilon_{xxxx} \\ &\quad - 3\alpha_7^2 C_{xyyy}^{ix} \left(e^{\alpha_7 x} \int^x \epsilon_{xxxx}(\eta) e^{-\alpha_7 \eta} d\eta - e^{-\alpha_7 x} \int^x \epsilon_{xxxx}(\eta) e^{\alpha_7 \eta} d\eta \right) \\ &= \tau_{zz} \end{aligned} \quad (\text{B.20})$$

$$\tau_{xxx} = C_{xxx}^{xxx} \epsilon_{xxx} = 2(a_1 + a_2 + a_3 + a_4 + a_5) \epsilon_{xxx} \quad (\text{B.21})$$

$$\tau_{yyx} = C_{yyx}^{xxx} \epsilon_{xxx} = (a_2 + 2a_3) \epsilon_{xxx} = \tau_{zzx} \quad (\text{B.22})$$

$$\tau_{xyz} = 0 = \tau_{yzx} = \tau_{xzy} = \tau_{zxx} = \tau_{xxz} \quad (\text{B.23})$$

$$\tau_{xyy} = \frac{a_2 + 2a_1}{2} \epsilon_{xxx} = C_{xyy}^{xxx} \epsilon_{xxx} \quad (\text{B.24})$$

$$\tau_{xzz} = \frac{a_2 + 2a_1}{2} \epsilon_{xxx} = \tau_{xyy} \quad (\text{B.25})$$

$$\tau_{xyx} = C_{xyx}^{xxy} \epsilon_{xxy} + C_{xyx}^{xxxxy} \frac{\partial \epsilon_{xxxxy}}{\partial x} \quad (\text{B.26})$$

$$\tau_{xxy} = C_{xxy}^{xxy} \epsilon_{xxy} + C_{xxy}^{xxxxy} \frac{\partial \epsilon_{xxxxy}}{\partial x} \quad (\text{B.27})$$

with

$$\begin{aligned}
-2D_{345}C_{xyx}^{xxy} &= 4a_4a_5^2 - a_2a_5^2 + 2a_1a_5^2 - 4a_4^2a_5 + 9a_2a_4a_5 + 2a_1a_4a_5 \\
&\quad + 4a_1a_3a_5 - a_2^2a_5 - 8a_4^3 - 16a_3a_4^2 - 6a_2a_4^2 - 16a_1a_4^2 \\
&\quad - 28a_1a_3a_4 + 7a_2^2a_4
\end{aligned} \tag{B.28}$$

$$\begin{aligned}
4D_{345}C_{xyx}^{xxxxy} &= 8a_1a_5b_5 - 8a_2a_4b_5 - 8a_1a_4b_5 - 8a_1a_5b_4 + 8a_2a_4b_4 \\
&\quad + 8a_1a_4b_4 + a_2a_5b_3 - 2a_1a_5b_3 + 2a_2a_4b_3 - 4a_1a_3b_3 \\
&\quad + a_2^2b_3 - 8a_2a_5b_2 - 8a_1a_5b_2 + 8a_2a_4b_2 + 24a_1a_4b_2 \\
&\quad + 32a_1a_3b_2 - 8a_2^2b_2
\end{aligned} \tag{B.29}$$

$$\begin{aligned}
-2D_{345}C_{xxy}^{xxy} &= 4a_5^3 - 8a_4a_5^2 - 4a_3a_5^2 + 10a_2a_5^2 + 4a_1a_5^2 - 4a_4^2a_5 - 12a_3a_4a_5 \\
&\quad - 18a_2a_4a_5 - 16a_1a_4a_5 - 28a_1a_3a_5 + 7a_2^2a_5 + 8a_4^3 + 24a_3a_4^2 \\
&\quad + 4a_2a_4^2 + 12a_1a_4^2 + 36a_1a_3a_4 - 9a_2^2a_4
\end{aligned} \tag{B.30}$$

$$\begin{aligned}
4D_{345}C_{xxy}^{xxxxy} &= 8a_2a_5b_5 - 32a_3a_4b_5 - 8a_2a_4b_5 - 32a_1a_3b_5 + 8a_2^2b_5 - 8a_2a_5b_4 \\
&\quad + 32a_3a_4b_4 + 8a_2a_4b_4 + 32a_1a_3b_4 - 8a_2^2b_4 + 4a_3a_5b_3 - 2a_2a_5b_3 \\
&\quad + 8a_3a_4b_3 + 12a_1a_3b_3 - 3a_2^2b_3 - 32a_3a_5b_2 - 8a_2a_5b_2 \\
&\quad + 32a_3a_4b_2 + 24a_2a_4b_2
\end{aligned} \tag{B.31}$$

$$\begin{aligned}
D_{345} &= a_5^2 - a_4a_5 + 2a_2a_5 + a_1a_5 - 2a_4^2 - 4a_3a_4 - 2a_2a_4 - 3a_1a_4 \\
&\quad - 4a_1a_3 + a_2^2
\end{aligned} \tag{B.32}$$

and

$$\tau_{yyy} = 3C_{xyyy}^{xxy} \epsilon_{xxxxy} \tag{B.33}$$

$$\tau_{zzy} = 3C_{xzyy}^{xxy} \epsilon_{xxxxy} \tag{B.34}$$

$$\tau_{yzy} = 0 = \tau_{yyz} = \tau_{zzz} \tag{B.35}$$

$$\tau_{yzz} = 3C_{xyz}^{xxy} \epsilon_{xxxxy} \tag{B.36}$$

$$\tau_{xxyy} = \tau_{xxzz} \quad (\text{B.37})$$

$$\begin{aligned} &= C_{xxyy}^{xx} \epsilon_{xx} + C_{xxyy}^0 b_0 \\ &+ C_{xxyy}^{ix} \left(e^{\alpha_7 x} \int^x \epsilon_{xxxx}(\eta) e^{-\alpha_7 \eta} d\eta - e^{-\alpha_7 x} \int^x \epsilon_{xxxx}(\eta) e^{\alpha_7 \eta} d\eta \right) \end{aligned} \quad (\text{B.38})$$

with

$$\begin{aligned} C_{xxyy}^{xx} &= -\frac{(\lambda c_3 - 2\mu c_1)(3b_7 + 3b_6 + 2b_3 + 4b_2) - c_2 \lambda (4b_5 + 4b_4 + 2b_3 + 8b_1)}{6((\lambda + \mu)(3b_7 + 3b_6 + 4b_5 + 4b_4 + 4b_3 + 4b_2 + 8b_1) - (c_3 + c_2 + 2c_1)^2)} \\ &+ c_2 \frac{(\lambda + \mu)(6b_7 + 6b_6 + 8b_5 + 8b_4 + 8b_3 + 8b_2 + 16b_1)}{6((\lambda + \mu)(3b_7 + 3b_6 + 4b_5 + 4b_4 + 4b_3 + 4b_2 + 8b_1) - (c_3 + c_2 + 2c_1)^2)} \\ &+ c_2 \frac{-2(c_3 + c_2 + 2c_1)(c_3 + c_2 + 3c_1)}{6((\lambda + \mu)(3b_7 + 3b_6 + 4b_5 + 4b_4 + 4b_3 + 4b_2 + 8b_1) - (c_3 + c_2 + 2c_1)^2)} \end{aligned} \quad (\text{B.39})$$

$$C_{xxyy}^0 = \frac{(\lambda + \mu)(3b_7 + 3b_6 + 2b_3 + 4b_2) - c_2(c_3 + c_2 + 2c_1)}{3((\lambda + \mu)(3b_7 + 3b_6 + 4b_5 + 4b_4 + 4b_3 + 4b_2 + 8b_1) - (c_3 + c_2 + 2c_1)^2)} \quad (\text{B.40})$$

$$C_{xxyy}^{ix} = \frac{G_\epsilon}{2\alpha_7} \quad (\text{B.41})$$

$$\begin{aligned} \tau_{xxxx} &= C_{xxxx}^{xx} \epsilon_{xx} + C_{xxxx}^{xxxx} \epsilon_{xxxx} + C_{xxxx}^0 b_0 \\ &+ C_{xxxx}^{ix} \left(e^{\alpha_7 x} \int^x \epsilon_{xxxx}(\eta) e^{-\alpha_7 \eta} d\eta - e^{-\alpha_7 x} \int^x \epsilon_{xxxx}(\eta) e^{\alpha_7 \eta} d\eta \right) \end{aligned} \quad (\text{B.42})$$

where

$$\begin{aligned}
Q_{xxxx}^{xx} C_{xxxx}^{xx} &= (\lambda + \mu)(c_2 + c_3)(3b_7 + 3b_6 + 4b_5 + 4b_4 + 4b_3 + 4b_2 + 8b_1) \\
&\quad + \mu c_1(3b_7 + 3b_6 + 4b_5 + 4b_4 + 4b_3 + 4b_2) \\
&\quad + (c_3 + c_2)(4b_1\lambda - (c_3 + c_2 + 2c_1)(c_3 + c_2 + 3c_1)) \quad (B.43)
\end{aligned}$$

$$\begin{aligned}
Q_{xxxx}^{xxxx} C_{xxxx}^{xxxx} &= 2c_3((b_7 + b_6)(3b_7 + 3b_6 + 3b_5 + 3b_4 + 5b_3 + 7b_2 + 3b_1) \\
&\quad + 2(b_3 + 2b_2)(b_5 + b_4 + b_3 + b_2 + 3b_1)) \\
&\quad + 2c_1(b_7 + b_6)(6b_7 + 6b_6 + 6b_5 + 6b_4 + 7b_3 + 8b_2) \\
&\quad - 4c_2((b_7 + b_6)(2b_5 + 2b_4 + b_3 + 4b_1) \\
&\quad + (b_5 + b_4 + b_3 + b_2 + 3b_1)(2b_5 + 2b_4 + b_3)) \quad (B.44)
\end{aligned}$$

$$\begin{aligned}
C_{xxxx}^0 &= \quad (B.45) \\
&\quad \frac{(\lambda + \mu)(3b_7 + 3b_6 + 4b_5 + 4b_4 + 4b_3 + 4b_2) - (c_3 + c_2)(c_3 + c_2 + 2c_1)}{(\lambda + \mu)(3b_7 + 3b_6 + 4b_5 + 4b_4 + 4b_3 + 4b_2 + 8b_1) - (c_3 + c_2 + 2c_1)^2}
\end{aligned}$$

$$\begin{aligned}
C_{xxxx}^{ix} &= \quad (B.46) \\
&\quad \frac{-6G_\epsilon(4b_1(c_3 + c_2) - c_1(3b_7 + 3b_6 + 4b_5 + 4b_4 + 4b_3 + 4b_2))}{2\alpha_7((c_3 + 2c_1)(3b_7 + 3b_6 + 2b_3 + 4b_2) - c_2(4b_5 + 4b_4 + 2b_3 + 8b_1))}
\end{aligned}$$

$$\begin{aligned}
Q_{xxxx}^{xx} &= \quad (B.47) \\
&\quad (\lambda + \mu)(3b_7 + 3b_6 + 4b_5 + 4b_4 + 4b_3 + 4b_2 + 8b_1) - (c_3 + c_2 + 2c_1)^2
\end{aligned}$$

$$\begin{aligned}
Q_{xxxx}^{xxxx} &= \quad (B.48) \\
&\quad (c_3 + 2c_1)(3b_7 + 3b_6 + 2b_3 + 4b_2) - c_2(4b_5 + 4b_4 + 2b_3 + 8b_1)
\end{aligned}$$

$$\tau_{xyzx} = \tau_{xxzy} = \tau_{xyyz} = 0 \quad (B.49)$$

$$\tau_{xyzy} = \tau_{xzzz} = \tau_{xyyz} = 0 \quad (B.50)$$

$$\tau_{xzzy} = \frac{2b_5 - 2b_4 - b_3}{3} \epsilon_{xxxy} + \frac{b_0}{3} = C_{xzzy}^{xxxy} \epsilon_{xxxy} \quad (\text{B.51})$$

$$\tau_{yyyy} = \frac{2}{3}(b_5 - b_4 - 2b_2) \epsilon_{xxxy} = C_{yyyy}^{xxxy} \epsilon_{xxxy} \quad (\text{B.52})$$

$$\tau_{xyzz} = -\frac{2}{3}b_2 \epsilon_{xxxy} = C_{xyzz}^{xxxy} \epsilon_{xxxy} \quad (\text{B.53})$$

$$\begin{aligned} \tau_{xzzx} &= C_{xzzx}^{xx} \epsilon_{xx} + C_{xzzx}^{xxxx} \epsilon_{xxxx} + C_{xzzx}^0 b_0 \\ &+ C_{xzzx}^{ix} \left(e^{\alpha_7 x} \int^x \epsilon_{xxxx}(\eta) e^{-\alpha_7 \eta} d\eta - e^{-\alpha_7 x} \int^x \epsilon_{xxxx}(\eta) e^{\alpha_7 \eta} d\eta \right) \end{aligned} \quad (\text{B.54})$$

and

$$\begin{aligned} \tau_{xyyx} &= C_{xyyx}^{xx} \epsilon_{xx} + C_{xyyx}^{xxxx} \epsilon_{xxxx} + C_{xyyx}^0 b_0 \\ &+ C_{xyyx}^{ix} \left(e^{\alpha_7 x} \int^x \epsilon_{xxxx}(\eta) e^{-\alpha_7 \eta} d\eta - e^{-\alpha_7 x} \int^x \epsilon_{xxxx}(\eta) e^{\alpha_7 \eta} d\eta \right) \end{aligned} \quad (\text{B.55})$$

with

$$C_{xyyx}^{xx} = \frac{\lambda(c_3(6b_7 + 6b_6 + 8b_5 + 8b_4 + 10b_3 + 12b_2 + 24b_1) - c_2(3b_7 + 3b_6 + 4b_5 + 4b_4 + 2b_3))}{6((\lambda + \mu)(3b_7 + 3b_6 + 4b_5 + 4b_4 + 4b_3 + 4b_2 + 8b_1) - (c_3 + c_2 + 2c_1)^2)} + \frac{\mu(c_3(6b_7 + 6b_6 + 8b_5 + 8b_4 + 8b_3 + 8b_2 + 16b_1) + c_1(6b_7 + 6b_6 + 8b_5 + 8b_4 + 4b_3))}{6((\lambda + \mu)(3b_7 + 3b_6 + 4b_5 + 4b_4 + 4b_3 + 4b_2 + 8b_1) - (c_3 + c_2 + 2c_1)^2)} - \frac{2c_3(c_3 + c_2 + 2c_1)(c_3 + c_2 + 3c_1)}{6((\lambda + \mu)(3b_7 + 3b_6 + 4b_5 + 4b_4 + 4b_3 + 4b_2 + 8b_1) - (c_3 + c_2 + 2c_1)^2)} \quad (\text{B.56})$$

$$C_{xyyx}^{xxxx} = \frac{c_3((2b_5 + 2b_4 + b_3 + 2b_1)(3b_7 + 3b_6 + 2b_3 + 4b_2) + 2(b_3 + 2b_2)(b_3 + 2b_2 + 4b_1))}{3((c_3 + 2c_1)(3b_7 + 3b_6 + 2b_3 + 4b_2) - 2c_2(2b_5 + 2b_4 + b_3 + 4b_1))} + \frac{-c_2(3(b_3 + 2b_2 + 2b_1)(b_7 + b_6) + 4(2b_5 + 2b_4 + b_3)(b_5 + b_4 + b_3 + b_2 + 3b_1))}{3((c_3 + 2c_1)(3b_7 + 3b_6 + 2b_3 + 4b_2) - 2c_2(2b_5 + 2b_4 + b_3 + 4b_1))} + \frac{12(b_5 + b_4 - b_2)(b_7 + b_6)c_1}{3((c_3 + 2c_1)(3b_7 + 3b_6 + 2b_3 + 4b_2) - 2c_2(2b_5 + 2b_4 + b_3 + 4b_1))} \quad (\text{B.57})$$

$$C_{xyyx}^0 = \frac{(\lambda + \mu)(3b_7 + 3b_6 + 4b_5 + 4b_4 + 2b_3) - c_3(c_3 + c_2 + 2c_1)}{3((\lambda + \mu)(3b_7 + 3b_6 + 4b_5 + 4b_4 + 4b_3 + 4b_2 + 8b_1) - (c_3 + c_2 + 2c_1)^2)} \quad (\text{B.58})$$

$$C_{xyyx}^{ix} = \frac{-G_\epsilon(c_3(2b_3 + 4b_2 + 8b_1) - (c_2 + 2c_1)(3b_7 + 3b_6 + 4b_5 + 4b_4 + 2b_3))}{2\alpha_7((c_3 + 2c_1)(3b_7 + 3b_6 + 2b_3 + 4b_2) - c_2(4b_5 + 4b_4 + 2b_3 + 8b_1))} \quad (\text{B.59})$$

$$C_{zzzz}^{xx} = \frac{2\lambda c_3(b_3 + 2b_2 + 4b_1) + (2c_1\mu - c_2\lambda)(3b_7 + 3b_6 + 4b_5 + 4b_4 + 2b_3)}{6((\lambda + \mu)(3b_7 + 3b_6 + 4b_5 + 4b_4 + 4b_3 + 4b_2 + 8b_1) - (c_3 + c_2 + 2c_1)^2)} + \frac{c_3(\lambda + \mu)(6b_7 + 6b_6 + 8b_5 + 8b_4 + 8b_3 + 8b_2 + 16b_1)}{6((\lambda + \mu)(3b_7 + 3b_6 + 4b_5 + 4b_4 + 4b_3 + 4b_2 + 8b_1) - (c_3 + c_2 + 2c_1)^2)} \quad (\text{B.60})$$

$$C_{zzzz}^{xx} = \frac{2c_3(c_3 + c_2 + 2c_1)(c_3 + c_2 + 3c_1)}{6((\lambda + \mu)(3b_7 + 3b_6 + 4b_5 + 4b_4 + 4b_3 + 4b_2 + 8b_1) - (c_3 + c_2 + 2c_1)^2)} \quad (\text{B.61})$$

$$C_{zzzz}^{xxxx} = \frac{c_3(3(b_7 + b_6)(2b_5 + 2b_4 + b_3 + 2b_1) + 4(b_3 + 2b_2)(b_5 + b_4 + b_3 + b_2 + 3b_1))}{3((c_3 + 2c_1)(3b_7 + 3b_6 + 2b_3 + 4b_2) - c_2(4b_5 + 4b_4 + 2b_3 + 8b_1))} + \frac{-c_2(3(b_7 + b_6)(b_3 + 2b_2 + 2b_1) + 4(b_5 + b_4 + b_3 + b_2 + 3b_1)(2b_5 + 2b_4 + b_3))}{3((c_3 + 2c_1)(3b_7 + 3b_6 + 2b_3 + 4b_2) - c_2(4b_5 + 4b_4 + 2b_3 + 8b_1))} + \frac{12c_1(b_5 + b_4 - b_2)(b_7 + b_6)}{3((c_3 + 2c_1)(3b_7 + 3b_6 + 2b_3 + 4b_2) - c_2(4b_5 + 4b_4 + 2b_3 + 8b_1))} \quad (\text{B.62})$$

$$C_{zzzz}^0 = C_{xyyx}^0 \quad (\text{B.63})$$

$$C_{zzzz}^{ix} = \frac{-G_\epsilon(c_3(2b_3 + 4b_2 + 8b_1) - (c_2 + 2c_1)(3b_7 + 3b_6 + 4b_5 + 4b_4 + 2b_3))}{2\alpha_7((c_3 + 2c_1)(3b_7 + 3b_6 + 2b_3 + 4b_2) - c_2(4b_5 + 4b_4 + 2b_3 + 8b_1))} \quad (\text{B.64})$$

$$C_{zzzz}^{ix} = \frac{-G_\epsilon(c_3(2b_3 + 4b_2 + 8b_1) - (c_2 + 2c_1)(3b_7 + 3b_6 + 4b_5 + 4b_4 + 2b_3))}{2\alpha_7((c_3 + 2c_1)(3b_7 + 3b_6 + 2b_3 + 4b_2) - c_2(4b_5 + 4b_4 + 2b_3 + 8b_1))} \quad (\text{B.65})$$

$$\tau_{zzzx} = 0 = \tau_{yyzx} = \tau_{xxzx} = \tau_{xxxx} \quad (\text{B.66})$$

$$\tau_{yyyy} = C_{yyyy}^{xxxx} \epsilon_{xxxx} = -(b_3 - 2b_4 + 2b_5) \epsilon_{xxxx} \quad (\text{B.67})$$

$$\tau_{yzzx} = C_{yzzx}^{xxxx} \epsilon_{xxxx} = -\frac{3b_3 - 2\sqrt{6}b_4 + 2\sqrt{6}b_5}{3\sqrt{6}} \epsilon_{xxxx} \quad (\text{B.68})$$

$$\tau_{xxyx} = C_{xxyx}^{xxxx} \epsilon_{xxxx} = -\frac{1}{3}(4b_2 + b_3 - 2b_4 + 2b_5 + 6b_6 + 2b_7) \epsilon_{xxxx} \quad (\text{B.69})$$

$$\tau_{xxxy} = C_{xxxy}^{xxxx} \epsilon_{xxxx} = -(b_3 + 2b_4 - 2b_5 - 2b_6 + 2b_7) \epsilon_{xxxx} \quad (\text{B.70})$$

Appendix C. Optimal constitutive equations for Cauchy materials

This appendix details for the sake of clarity the approach proposed in Sect.3 when applied to Cauchy materials. The Euler-Bernoulli kinematic assumption reads

$$\epsilon_{xx} = -y \frac{d^2v}{dx^2} + \frac{du}{dx} \quad (\text{C.1})$$

and the static admissibility conditions impose that

$$\tau_{yz} = \tau_{yy} = \tau_{zz} = 0 \quad (\text{C.2})$$

The stresses resulting from the 3D law read :

$$\tau_{xx} = (\lambda + 2\mu) \epsilon_{xx} \quad (\text{C.3})$$

$$\tau_{yy} = \tau_{zz} = \lambda \epsilon_{xx} \quad (\text{C.4})$$

Using the 3D constitutive law thus makes the tensile stiffness wrong and violates the static admissibility conditions (C.2), thereby making the need for a modified constitutive law explicit. Under the assumptions (C.1) and

(C.2), $\eta_\psi(\mathbf{T}, \mathbf{E}_{KA})$ satisfies

$$\begin{aligned} E\eta_\psi(\mathbf{T}, \mathbf{E}_{KA}) &= \tau_{xx}^2 + 2(1 + \nu)(\tau_{xy}^2 + \tau_{xz}^2) + \epsilon_{xx}\tau_{xx}(2(2\nu - 1)\lambda - 4\mu) \quad (\text{C.5}) \\ &\quad + \epsilon_{xx}^2((\lambda + 2\mu)(\lambda + 2\mu - 2\nu\lambda) + 2\lambda(\lambda(1 + \nu) - \nu(3\lambda + 2\mu))) \end{aligned}$$

The stationarity of $\eta_\psi(\mathbf{T}, \mathbf{E}_{KA})$ with respect to the stress components (see Eq.43) $\tau_{xx}, \tau_{xy}, \tau_{xz}$ yields :

$$\begin{aligned} \tau_{xx} &= E\epsilon_{xx} \\ \tau_{xy} &= 0 \\ \tau_{xz} &= 0 \end{aligned} \quad (\text{C.6})$$

so that the constitutive equations usually considered for beam equations are recovered instead of the 3D constitutive law. The equations (C.6) yield \mathbf{T}_{SA} . The minimal constitutive equation gap reads

$$E\eta_\psi(\mathbf{T}_{SA}, \mathbf{E}_{KA}) = E\epsilon_{xx}^2 \frac{2\nu^2}{(1 + \nu)(1 - 2\nu)} > 0 \quad (\text{C.7})$$

As a consequence of the constitutive equation gap, the strain energy may be assessed either using the kinematic fields or the static ones, yielding different values. The quality of the solution (C.6) may be approached by the scaled residual constitutive equation gap :

$$\frac{\eta_\psi(\mathbf{T}_{SA}, \mathbf{E}_{KA})}{\mathbf{E}_{KA} \cdot \mathcal{C} \cdot \mathbf{E}_{KA} + \mathbf{T}_{SA} \cdot \mathcal{C}^{-1} \cdot \mathbf{T}_{SA}} = \frac{\nu^2}{(1 - \nu) - \nu^2} \quad (\text{C.8})$$

which is found to be rather large when $\nu \rightarrow \frac{1}{2}$. The residual constitutive equation gap may be further analyzed by defining a modified constitutive equation gap $\bar{\eta}_\psi(\mathbf{T}, \mathbf{E})$

$$\bar{\eta}_\psi(\mathbf{T}, \mathbf{E}) = (\mathbf{T} - \mathcal{C} \cdot \mathbf{E}) \cdot \mathcal{C}^{-1} \bar{\mathcal{C}} \cdot \mathcal{C}^{-1} \cdot (\mathbf{T} - \mathcal{C} \cdot \mathbf{E}) \quad (\text{C.9})$$

where $\bar{\mathcal{C}}$ is the stiffness operator in which all the components related to the strain components in the cross-section have been zeroed. It can be checked that

$$\bar{\eta}_\psi(\mathbf{T}_{SA}, \mathbf{E}_{KA}) = 0 \quad (\text{C.10})$$

thereby proving that the residual constitutive equation gap is solely located in these in-plane deformation components. The other strain components may thus be considered as accurate, even though the global error indicator (C.8) turns to be rather high.

Appendix D. First strain gradient elasticity for the bending problem

Neglecting any term related to the second-strain gradient in Eq. (90) yields the characteristic equation

$$-\frac{t^2 C_{xxx}^{xxx}}{12} \frac{d^6 v}{dx^6} + K \frac{d^4 v}{dx^4} = 0 \quad \forall x \in [0, L] \quad (\text{D.1})$$

One should first outline that as for bars, this differential equation is formally similar to the one obtained from a purely kinematic approach [47] in the absence of distributed loading :

$$g^2 \frac{d^6 v}{dx^6} - \left(1 + c \frac{g^2}{t^2}\right) \frac{d^4 v}{dx^4} = 0 \quad \forall x \in [0, L] \quad (\text{D.2})$$

and the this work provides the definition

$$c = \frac{12(C_{xxy}^{xxy} - 2C_{xyx}^{xxy})}{C_{xxx}^{xxx}} \quad (\text{D.3})$$

, again extending results obtained with a simplified constitutive equation [47, 43]. Looking for solutions of the form (73) yields

$$0 = \alpha_v^4 \left\{ -\frac{t^2 C_{xxx}^{xxx}}{12} \alpha_v^2 + K \right\} \quad (\text{D.4})$$

whose non-trivial solutions read

$$\alpha_v = \pm \lambda_V^{-1} \quad (\text{D.5})$$

with

$$\lambda_V = t \sqrt{\frac{C_{xxx}^{xxx}}{12K}} \quad (\text{D.6})$$

As seen in Fig.4, C_{xxx}^{xxx} is found to be always positive, as well as $C_{xxy}^{xxy} - 2C_{xyx}^{xxy}$ (see Fig. 11). The term K defined in Eq.(92) is thus always positive, so that λ_V is always a real number. The displacement field therefore reads

$$v(x) = q_0 + \sum_{i=1}^3 q_i \left(\frac{x}{iL} \right) + \gamma_{FSG}^+ \exp\left(\frac{x}{\lambda_V} \right) + \gamma_{FSG}^- \exp\left(-\frac{x}{\lambda_V} \right) \quad (\text{D.7})$$

6 boundary conditions are therefore necessary to set the solution. These are obtained from Eq.(68). Assuming the beam is clamped at $x = 0$, these boundary conditions read

$$\begin{aligned} v(0) &= 0 \\ \frac{dv}{dx}(0) &= 0 \\ -\frac{t^2 C_{xxx}^{xxx}}{12} \frac{d^3 v}{dx^3}(0) &= 0 \end{aligned}$$

A bending force F is applied at $x = L$, the work of external forces reads $\delta W^* = F v^*(x = L)$ so that

$$\begin{aligned} -\frac{t^2 C_{xxx}^{xxx}}{12} \frac{d^5 v}{dx^5}(L) + K \frac{d^3 v}{dx^3}(L) &= -\frac{F}{bt} \\ -\frac{t^2 C_{xxx}^{xxx}}{12} \frac{d^4 v}{dx^4}(L) + K \frac{d^2 v}{dx^2}(L) &= 0 \\ -\frac{t^2 C_{xxx}^{xxx}}{12} \frac{d^3 v}{dx^3}(L) &= 0 \end{aligned}$$

Solving the linear system above yields the tip displacement

$$\frac{btv^{FSG}(L)}{F} = \frac{12\lambda_V^2}{C_{xxx}} \left\{ \frac{L}{6t^2}(2L^2 - 3\lambda_V^2) + \frac{e^{\frac{L}{\lambda_V}} - 1}{e^{\frac{L}{\lambda_V}} + 1} \left(\frac{\lambda_V}{2t^2}(4\lambda_V^2 - L^2) + \frac{L^2 C_{xxx}}{24K\lambda_V} \right) \right\} \quad (D.8)$$

It can be checked that

$$\lim_{t \rightarrow +\infty} \frac{btv^{FSG}(L)}{F} = \frac{4L^3}{t^2 C_{xx}} \quad (D.9)$$

which corresponds to the solution for Cauchy materials :

$$\frac{K_V^{FSG}}{K_V^{Cauchy}} = \frac{4F L^3}{bt^3 v^{FSG}(L) C_{xx}} \quad (D.10)$$

and

$$\lim_{t \rightarrow +\infty} \frac{K_V^{FSG}}{K_V^{Cauchy}} = 1 \quad (D.11)$$

It is also worth noting that

$$\lim_{t \rightarrow +\infty} \lambda_V = \sqrt{\frac{C_{xxx}}{C_{xx}}} = \lambda_V^\infty \quad (D.12)$$

Considering the vanishing thickness limit, it is straightforward that λ_V then scales as the thickness :

$$\lambda_V \underset{t=0}{\propto} t \sqrt{\frac{C_{xxx}}{12(C_{xxy} - 2C_{xyx})}} \quad (D.13)$$

Appendix E. Material parameters for the reported results

References

- [1] Lam D.C.C., Yang F., Chong A.C.M., Wang J., Tong P. (2003) Experiments and theory in strain gradient elasticity. *J. Mech. Phys. Solids* 51:1477-1508.

Parameter	'blue' material	'green' material
λ (a.u.)	0.23450	0.89866
μ (a.u.)	0.32954	0.57411
$a_1 \times l_S^{-2}$	0.405576	0.422018
$a_2 \times l_S^{-2}$	0.455259	0.406719
$a_3 \times l_S^{-2}$	0.054128	0.346389
$a_4 \times l_S^{-2}$	0.360096	0.128259
$a_5 \times l_S^{-2}$	0.197339	0.084851
$b_1 \times l_S^{-4}$	0.381855	-0.072306
$b_2 \times l_S^{-4}$	0.312357	0.075082
$b_3 \times l_S^{-4}$	-0.147836	-0.185854
$b_4 \times l_S^{-4}$	0.083769	0.354568
$b_5 \times l_S^{-4}$	0.362985	0.296555
$b_6 \times l_S^{-4}$	0.439393	0.239330
$b_7 \times l_S^{-4}$	0.489509	0.385830
$c_1 \times l_S^{-2}$	-0.084471	0.118333
$c_2 \times l_S^{-2}$	-0.297773	0.448119
$c_3 \times l_S^{-2}$	-0.469331	-0.034367

- [2] Liebold C., Müller W.H. (2015) Applications of strain gradient theories to the size effect in submicro-structures incl. experimental analysis of elastic material parameters. Bulletin of TICMI 19(1):45-55.
- [3] Cuenot S., Frétiigny C., Demoustier-Champagne S., Nysten B. (2004) Surface tension effect on the mechanical properties of nanomaterials measured by atomic force microscopy. Phys. Rev. B 69:165410.

- [4] Ren Y., Lam D.C.C (2005) Experiments on the elastic size dependence of LPCVD silicon nitride. *Mater. Res. Soc. Symp. Proc.* 875.
- [5] Berger R., Delamarche E., Lang H. P., Gerber C., Gimzewski J.K., Meyer E., Güntherodt H.-J. (1997) Surface stress in the self-assembly of alkanethiols on gold. *Science* 276:2021-2024.
- [6] Boisen A., Dohn S., Keller S.S., Schmid S., Tenje M. (2011) Cantilever-like micromechanical sensors. *Reports on Progress in Physics* 74(3):036101.
- [7] Khakalo S., Balobanov V., Niiranen J. (2018) Modelling size-dependent bending, buckling and vibrations of 2D triangular lattices by strain gradient elasticity models: applications to sandwich beams and auxetics. *International Journal of Engineering Science*, 127, 33-52.
- [8] Khakalo S., Niiranen J. (2019) Lattice structures as thermoelastic strain gradient metamaterials: Evidence from full-field simulations and applications to functionally step-wise-graded beams. *Composites Part B: Engineering*, 177, 107224.
- [9] Thai H.-T., Vo T.P., Nguyen T.-K., Kim S.-E. (2017) A review of continuum mechanics models for size-dependent analysis of beams and plates. *Composite structures* 177: 196-219
- [10] Gurtin M.E., Markenscoff X., Thurston R.N. (1976) Effect of surface stress on the natural frequency of thin crystals. *Appl. Phys. Lett.* 29(9):529-530.

- [11] Gurtin M. E., Murdoch A. I. (1978) Surface stress in solids. *Int. J. Solids Structures* 14:431-440.
- [12] Begley M.R., Utz M., Komaragiri U. (2005) Chemo-mechanical interactions between adsorbed molecules and thin elastic films. *Journal of the Mechanics and Physics of Solids* 53:2119-2140.
- [13] Begley M.R., Utz M. (2008) Multiscale modeling of adsorbed molecules on freestanding microfabricated structures. *Jal. Appl. Mech.* 75.
- [14] Amiot F. (2007) A model for chemically-induced mechanical loading on MEMS. *J. Mechanics of Materials and Structures* 2(9):1787-1803.
- [15] Neukirch S., Antkowiack A., Marigo J.-J. (2013) The bending of an elastic beam by a liquid drop: a variational approach. *Proceedings of the Royal society A: Mathematical, physical and engineering sciences* 469(2157).
- [16] Rogula D. (1982) Introduction to Nonlocal Theory of Material Media. In: Rogula D. (eds) *Nonlocal Theory of Material Media*. International Centre for Mechanical Sciences (Courses and Lectures), vol 268. Springer, Vienna.
- [17] Lorentz E., Andrieux S. (2003) Analysis of non-local models through energetic formulations. *Int. J. Solids Structures* 40:2905-2936.
- [18] Mindlin R.D. (1964) Micro-structure in linear elasticity. *Arch. Rat. Mech. Anal.* 16(1): 51-78.

- [19] Mindlin R.D. (1965) Second gradient theory of strain and surface tension in linear elasticity. *Int. J. Solids Structures* 1:417-438.
- [20] Style R.W., Jagota A., Hui C.-Y., Dufresne E.R. (2017) Elastocapillarity: surface tension and the mechanics of soft solids. *Annual Review of Condensed Matter Physics* 8:99-118.
- [21] Polizzotto C. (2013) A second strain gradient theory with second velocity gradient inertia - Part 1: constitutive equations and quasi-static behavior. *Int. J. Solids Structures* 50:3749-3765.
- [22] Ojaghnezhad F., Shodja H.M. (2016) Surface elasticity revisited in the context of second strain gradient theory. *Mechanics of materials* 93:220-237.
- [23] Cordero N.M., Forest S., Busso E.P. (2016) Second-strain gradient elasticity of nano-objects. *J. Mech. Phys. Solids* 97:92-124.
- [24] Khakalo S., Niiranen J. (2018) Form II of Mindlin's second strain gradient theory of elasticity with a simplification: for materials and structures from nano- to macro-scales; *European Journal of Mechanics - A/Solids* 71, 292-319.
- [25] Vardoulakis I., Exadaktylos G., Kourkoulis S.K. (1998) Bending of marble with intrinsic length scales: a gradient theory with surface energy and size effects. *J. Phys. IV* 8:399-406.
- [26] Wang Q., Liew K.M. (2007) Application of nonlocal continuum mechanics to static analysis of micro- and nano-structures. *Physics Letters A* 363:236-242.

- [27] Papargyri-Beskou S., Beskos D. (2010) Static analysis of gradient elastic bars, beams, plates and shells. *The Open Mechanics journal* 4:65-73.
- [28] Ramezani S. (2012) A micro scale geometrically non-linear Timoshenko beam model based on strain gradient elasticity theory. *Int. Jal. Non-linear Mech.* 47:863-873.
- [29] Challamel N. (2013) Variational formulation of gradient or/and nonlocal higher-order shear elasticity beams. *Composite Structures* 105:351-368.
- [30] Liebold C., Müller W.H. (2016) Comparison of gradient elasticity models for the bending of micromaterials. *Computational Materials Science* 116:52-61.
- [31] Challamel N., Wang C.M. (2008) The small length scale effect for a non-local cantilever beam: a paradox solved. *Nanotechnology* 19:345703.
- [32] Lurie S., Solyaev Y. (2018) Revisiting bending theories of elastic gradient beams. *Int. Jal. Eng. Sci.* 126:1-21.
- [33] Amiot F. (2013) An Euler-Bernoulli second strain gradient beam theory for cantilever sensors. *Philosophical Magazine Letters* 93(4):204-212.
- [34] Karparvarfard S.M.H., Asghari M., Vatanikhak R. (2015) A geometrically nonlinear beam model based on the second strain gradient theory. *Int. Jal. Eng. Sci.* 91:63-75.
- [35] Dehrouyeh-Semnani A.M., Nikkhah-Bahrami M. (2015) A discussion on incorporating the Poisson effect in microbeam models based on modified couple stress theory. *Int. Jal. Eng. Sci.* 86:20-25.

- [36] Lazar M., Maugin G.A., Aifantis E.C. (2006) Dislocations in second strain gradient elasticity. *Int. J. Solids Structures* 43(6):1787-1817.
- [37] Mousavi S.M., Paavola J. (2014) Analysis of plate in second strain gradient elasticity. *Arch. Appl. Mech.* 84(8):1135-1143.
- [38] Yu W., Hodges D.H. (2004) Elasticity solutions versus asymptotic sectional analysis of homogeneous, isotropic, prismatic beams. *Jal. Appl. Mech.* 71: 15-23.
- [39] Ladevèze P. and Leguillon D. (1983). Error estimate procedure in the finite element method and applications. *SIAM J. Numer. Anal.* 20(3):485-509.
- [40] Ojaghnezhad F., Shodja H.M. (2013) A combined first principles and analytical determination of the modulus of cohesion, surface energy, and the additional constants in the second strain gradient elasticity. *Int. J. Solids Structures* 50:3967-3974.
- [41] Shodja H.M., Ahmadpoor F., Tehranchi A. (2012) Calculation of the additional constants for fcc materials in second strain gradient elasticity: behavior of a nano-size Bernoulli-Euler beam with surface effects. *Jal. Appl. Mech.* 79.
- [42] Niiranen J., Khakalo S., Balabanov V., Niemi A. H. (2016) Variational formulation and isogeometric analysis of fourth-order boundary value problems of gradient-elastic bar and plane strain/stress problems. *Computer Methods in Applied Mechanics and Engineering*, 308, 182-211.

- [43] Altan B.S., Aifantis E.C. (1997) On some aspects in the special theory of gradient elasticity. *J. Mech. Behav. Mater.* 8, 231-282.
- [44] Maranganti R., Sharma P. (2007) Length scales at which classical elasticity breaks down for various materials. *Phys. Rev. Lett.* 98:195504.
- [45] Maranganti R., Sharma P. (2007) A novel atomistic approach to determine strain-gradient elasticity constants: tabulation and comparison for various metals, semiconductors, silica, polymers and the (ir) relevance for nanotechnologies. *J. Mech. Phys. Solids* 55:1823-1852.
- [46] Jakata K, Every A.G. (2008) Determination of the dispersive elastic constants of the cubic crystals Ge, Si, GaAs and InSb. *Phys. Rev. B* 77:174301.
- [47] Niiranen J., Balobanov V., Kiendl J., Hosseini S. B. (2019) Variational formulations, model comparisons and numerical methods for Euler-Bernoulli micro- and nano-beam models. *Mathematics and Mechanics of Solids* 24, 312-335.
- [48] Press W.H., Teukolsky S.A., Vetterling W.T., Flannery B.P. (2002) *Numerical Recipes in C++*, Cambridge University Press, Cambridge (UK).